Ms#201011077, 8th of June, 2011

FGF and retinoic acid activity gradients control the timing of neural crest cell emigration in the trunk

Patricia L. Martínez-Morales[1], Ruth Diez del Corral[1], Isabel Olivera-Martínez[2], Alejandra C. Quiroga[1], Raman M. Das[2], Julio A. Barbas[1], Kate G. Storey[2] and Aixa V. Morales[1]

[1]Instituto Cajal, CSIC, Doctor Arce 37, 28002 Madrid, Spain.

[2] College of Life Science, University of Dundee, WTB, Dow Street, Dundee DD1 5EH, Scotland, UK

Characters: 40046

Running head: FGF and RA control neural crest cells emigration

eTOC Summary Statement: FGF acts as positional cues that prevents premature neural crest cell specification and EMT caudally while at the same time retinoic acid promotes EMT rostrally.

P.L. Martínez-Morales and R. Diez del Corral, contributed equally to this paper.

Correspondence to Aixa V. Morales: Instituto Cajal, CSIC, Doctor Arce 37, 28002 Madrid, Spain; tel. +34-915854722; fax: +34-915854754; aixamorales@cajal.csic.es

I. Olivera-Martínez present address is: CNRS UMR7622, Université Pierre et Marie Curie, 9 Quai St Bernard, 75252 Paris Cedex 05, France

Abstract

Coordination between functionally related adjacent tissues is essential during development. For example, formation of trunk neural crest cells is highly influenced by the adjacent mesoderm, but the molecular mechanism involved is not well understood. As part of this mechanism, FGF and retinoic acid (RA) mesodermal gradients control the onset of neurogenesis in the extending neural tube. Now, using gain- and loss-of-function experiments, we show that caudal FGF signaling prevented premature specification of neural crest cells and consequently premature epithelial-mesenchymal transition (EMT) in order to allow cell emigration. By contrast, rostrally generated RA promoted EMT of neural crest cells at somitic levels. Furthermore, we show that FGF and RA signaling controlled EMT in part through modulation of elements of the BMP and Wnt signaling pathways. These data establish a clear role for opposition of FGF and RA signaling in control of the timing of neural crest cell EMT and emigration and consequently coordination of the development of central and peripheral nervous system during vertebrate trunk elongation.

Introduction

The neural crest is formed by a transient population of multipotent cells that arise from the dorsal neural tube. Once specified, neural crest cells (NCC) undergo a process of epithelium to mesenchyme transition (EMT) that confers the ability to delaminate and migrate away from the dorsal neural tube. The NCCs migrate along characteristic pathways to differentiate into a wide variety of derivatives according to their rostro-caudal (R-C) position in the neural tube and the order of emigration (Krispin et al., 2010). NCC derivatives include craniofacial skeleton, sensory neurons and glia, sympathetic neurons and melanocytes, amongst others (Le Douarin and Kalcheim, 1999).

The process of neural crest formation implies the orchestration of a complex gene regulatory network (Morales et al., 2005; Sauka-Spengler and Bronner-Fraser, 2008). It involves signaling pathways and transcription factors that are responsible for the sequence of early induction of the NCC during gastrulation [Wnt, bone morphogenetic proteins (BMPs), fibroblast growth factor (FGF) and retinoic acid (RA); Saint-Jeannet et al, 1997; Liem et al., 1995; Monsoro-Burq et al., 2003; Villanueva et al., 2002]; the specification of the neural plate border (*Msx1/2, Pax3, Pax7* and *Zic1/3*; Liem et al., 1995; Brewester et al., 1998; Nakata et al., 1997); the expression of *bona fide* NCC transcription factors (*AP2*, *Snail*, *FoxD3*, *Sox5*, *Sox9* and *Sox10*; Barrallo-Gimeno et al., 2004; Nieto et al., 1994; Dottori et al 2001; Kos et al., 2001; Perez-Alcalá et al., 2004; Cheung and Briscoe, 2003; Paratore et al., 2001) and the regulation of numerous downstream effectors involved in cell adhesion and cell cycle control, amongst others (Sauka-Spengler and Bronner-Fraser, 2008).

Several neural crest specifier genes are co-expressed with neural plate border specifiers at early stages during gastrulation, suggesting possible early regulatory

relationships (Khudyakov and Bronner-Fraser; 2009). However, this early population of neural crest progenitors mostly represents the cephalic NCCs whereas the trunk neural crest progenitors will progressively be specified as the trunk neural tube elongates (Le Douarin and Kalcheim, 1999). In that sense, the role of BMP, FGF and Wnt signaling in the early NC induction has been derived from work in *Xenopus* at cephalic NC territory. Thus, the signals promoting trunk neural crest specification has not been fully elucidated.

The development of trunk NCCs is highly coordinated with the development of adjacent territories functionally related. In particular, flanking the neural tube, the paraxial or presomitic mesoderm (PSM) gets progressively segmented into smaller units, somites, and this metamerization imposes a segmented organization to the trunk NCCs. First, opposite the presomitic mesoderm, NCCs are confined to the dorsal neural tube whereas NCC emigration begins facing epithelial somites (Teillet et al., 1987; Sela-Donenfeld and Kalcheim, 1999). Moreover, the first indication of peripheral nervous system segmentation is the patterned ventral migration of NCCs through the anterior part of each somitic sclerotome (Tosney, 1978; Rickmann et al., 1985; Bronner-Fraser, 1986; Loring and Erickson, 1987).

There is little knowledge about the integration of signals involved in trunk NCC emigration. At trunk level, it has been shown that a BMP-Wnt1 signaling cascade controls NCC emigration (Sela-Donenfeld and Kalcheim, 1999; Burstyn-Cohen et al., 2004). The regulation of that cascade is exerted through the caudal (high)- rostral (low) gradient of the BMP inhibitor Noggin, which in turn is controlled by undetermined signals coming from somites (Sela-Donenfeld and Kalcheim, 2000).

In the paraxial mesoderm the FGF and RA pathways operate as a signaling switch that controls the R-C sequence of mesodermal and neural development. Opposite

gradients of declining caudal FGF and rostral RA signaling in the extending body axis create a wavefront which determines the onset of neuronal differentiation and patterning in newly generated spinal cord (Diez del Corral et al., 2002; Diez del Corral et al., 2003) and also position somite boundaries (Dubrulle et al., 2001; Diez del Corral et al., 2003). The trunk neural tube is generated during a long period of time as the main body axis extends caudally and trunk neural crest is also generated following this R-C sequence. Thus, FGF and RA signaling pathways are candidates to coordinate NCC development with somite and neuron formation as the embryo elongates.

In this work, using both gain- and loss-of-function approaches, we have established that FGF signaling through the MAPK pathway prevents the initiation of trunk NCC specification and consequently, neural crest cells EMT. By contrast, RA signaling triggers the EMT of specified NCCs. Furthermore, we show that FGF and RA signaling control the timing of EMT and emigration in part through modulation of elements of the BMP and Wnt signaling pathways. Thus, opposition of FGF and RA signaling orchestrates the onset of trunk NCC specification and emigration, coordinating them with somite formation and neurogenesis in the extending vertebrate body axis.

Results

Onset of NCC markers expression coincides with FGF8 decline

To investigate whether the paraxial mesoderm has a general influence on NCC specification and migration in the spinal cord, we compared the expression patterns of a cohort of genes involved in dorsal patterning and NCC specification with respect to the formation of somites in chicken embryos at Hamburger and Hamilton (HH) stages 10-14 (Fig. 1A-H). At HH10 stage, the caudal open neural plate expressed dorsal patterning genes such as *Pax7* (Kawakami et al., 1997; Fig. 1A), *Pax3* (Goulding et al., 1991; data not shown), *RhoB* (Liu et al., 1995; data not shown) and *Msx1* (Liem et al., 1995; data not shown). This expression is maintained along the neural tube as the body axis extends (Fig. 1A). More rostrally, when the neural folds move toward the midline to fuse, the expression of the NCC marker *Snail2* (Nieto et al., 1994) was found in the dorsal neural folds (Fig. 1B) adjacent to mid-PSM level. Subsequently, expression of *Sox* family genes involved in NCC formation could be observed in the dorsal neural tube. First, *Sox9* (Cheung et al., 2003; Fig. 1C) appeared rostral to the initiation of *Snail2* and then *Sox5* (Perez-Alcala et al., 2004; Fig. 1D). Finally, adjacent to forming somites, *Sox10* (Paratore et al., 2001; Fig. 1E) was observed in premigratory NCCs about to emigrate.

This order in the expression of the genes described is maintained throughout stages HH12-14 (data not shown). However, at HH10 *FoxD3,* a NCC specifier (Stewart et al., 2006), was not expressed dorsally in the neural folds (Fig. 1F). Only by HH12, *FoxD3* mRNA could be observed at rostral PSM level (Fig. 1G).

The initiation of the expression of NCC markers seems to coincide with the transition zone where neural progenitors stop expressing caudal neural markers and initiate ventral patterning gene expression. This transition is governed by the opposing

activities of the FGF and RA signaling gradients (Diez del Corral et al., 2003). In fact, by *in situ* hybridization of half embryos, we showed that the onset of *Snail2* expression coincided with the decline of the caudal neural gene *Sax1* expression (Bertrand et al. 2000; Fig. 1H) and the appearance of the ventral patterning gene *Pax6* (Bertrand et al. 2000; Fig. 1I). Moreover, the initiation of *Snail2* expression is close to the decay of *FGF8* transcripts in the neural tube (Fig. 1J) and high levels of *Snail2* mRNA coincided with the onset of the RA-synthesizing enzyme *Raldh2* expression in the adjacent mesoderm (Fig. 1K).

In summary, NCC markers are progressively transcribed in a precise temporal-spatial order in the presumptive region of premigratory NCCs. Moreover, these data suggest that the onset of specification and EMT of NCCs could be controlled by FGF and RA signaling gradients (summary in Fig. 1L).

FGF signaling controls the onset of trunk NCC specification through the MAPK pathway

FGF signaling is involved in the maintenance of the neural caudal stem zone and it also represses neuronal differentiation and ventral patterning (Bertrand et al., 2000; Diez del Corral et al., 2003). To determine if the onset of NCC specification was regulated by the decline of the caudal gradient of FGF8 signaling, we used the FGF receptor antagonist SU5402 (Mohammadi et al., 1997). Cultured HH11 embryos exposed to this drug for 4 hours exhibited a severe downregulation of the well-known FGF signaling target *Sprouty2* (Fig. 2B; n=13/13; Minowada et al., 1999) in comparison with control DMSO treated embryos (Fig. 2A; n=0/12). After 4 hours culture with SU5402, *Snail2* expression was enhanced in the dorsal part of the neural tube and prematurely initiated at the level of Hensen´s node (Fig. 2F; n=11/12) in comparison with control embryos

(Fig. 2E; n=4/18). A similar premature *Snail2* upregulation was observed using the specific FGFRI inhibitor PD173074 (Fig. S1; n=7/7; Skaper et al., 2000) and was quantified using qRT-PCR as a two-fold increase in relative *Snail2* mRNA levels in PD173074 with respect to DMSO treated samples in the neural tube at the level of the caudal PSM [2,06 (1,77-2,39); Fig. S1]. As a control, a similar qRT-PCR analysis showed a three-fold decrease in *Sprouty* relative mRNA levels in PD173074 with respect to DMSO treated samples (0,31±0,16; Fig. S1). PD173074 and SU5402 not only inhibit FGFR signaling but also target VEGFR (Mohammadi et al., 1997; Mohammadi et al., 1998). To determine whether these effects are specifically mediated by FGFR signalling we used a specific VEGFR inhibitor, KRN633 (Nakamura et al., 2004). This did not alter the onset of *Snail2* expression (Fig. S2, n=12/15) in relation to control DMSO treated embryos (Fig. S2, n=13/15). However, FGFRI inhibition either with PD173074 or SU5402 did not alter the expression of *FoxD3,* another NCC specifier (Fig. S1 and data not shown; n=4 and 7, respectively) with respect to control embryos (n=9). Together these results indicate that FGF caudal gradient prevents the premature expression of the early NCC specifier *Snail2* in the caudal neural tube.

Activation of the tyrosine kinase FGFR can initiate transduction via a number of downstream pathways including the mitogen-activated protein kinase (MAPK) and the phosphatidylinositol 3-kinase (PI3K; Schonwasser et al., 1998). Both pathways have been involved in the transmission of FGF signaling during early stages of neural development (Stavridis et al., 2007; Ribisi, Jr et al., 2000) and dual phosphorylated MAPK has been specifically detected in the caudal FGF signaling domain (Lunn et al., 2007). We investigated the potential role of the MEK/ERK regulatory pathway in the control of NCC specification, by selectively suppressing activation of MEK1 with the drug PD184352. In HH11-12 embryos cultured for 4 hours, this drug effectively

downregulated the expression of a direct target of FGF signaling *Sprouty2* (Fig. 2C; n=7/7) and reduced ERK1/2 phosphorylation (Fig. 2I; 92% decreased in phospho-ERK/ relative to total ERK; n=3) in comparison with DMSO treated embryos (Fig. 2A, I; n=6). As with inhibition of FGFRI, blockage of MAPK pathway leads to a premature and enhanced caudal expression of the NCC specifier *Snail2* (Fig. 2G; n=4/4). On the other hand, blockage of the PI3K pathway using the LY294002 treatment, that effectively reduces AKT phosphorylation (Fig. 2I; 73% decreased in phospho-AKT/ relative to total AKT; n=3), had very little effect on *Sprouty2* (Fig. 2D; n=1/7; Echevarria et al., 2005) and on *Snail2* mRNA expression (Fig. 2H; n=0/4). In conclusion, FGF signaling acting through the MAPK, but not the PI3K pathway, is required to prevent premature *Snail2* expression in NCCs, and consequently to delay NCC specification.

FGF signaling pathway controls the initiation of trunk NCC emigration

Premature specification of NCCs could lead to premature emigration at axial levels previous to somite formation. In the experiments described above, NCCs from embryos incubated with FGFRI inhibitors for 4 hours, that prematurely expressed *Snail2,* were not able to emigrate as assessed by the expression of *Sox10* (Fig. S1 and data not shown; n=9). To test better the consequence on NCC emigration, we examined the effect of blocking FGF signaling for longer periods of time using a dominant-negative FGFRI-EYFP protein (dn-FGFRI-EYFP; Yang et al., 2002) introduced into the right caudal hemitube at HH10-11. After 18-20 hours post electroporation, this construct blocked effectively the expression of FGF signaling targets such as *Sprouty2* (Fig. S3; n=7/9; Minowada et al., 1999) and induced *Pax6* expression (Fig. S3; n= 5/6; Bertrand et al., 2000) in the neural tube, in comparison with control pCIG embryos (Fig. S3; n= 6

and 4/5, respectively). Remarkably, dorsal neural progenitors expressing the dn-FGFRI-EYFP protein prematurely activated *Snail2* (data not shown; n=4/4) and *Sox10* expression and exited the neural tube (Fig. 3B; arrow; n=9/10) in comparison to the control side or to cells electroporated with a control EGFP (Fig. 3A; n=7). Moreover, the progressive disruption of the basal lamina, identified by Laminin expression (Martins-Green and Erickson, 1987), was also more advanced in the side where FGF signaling has been blocked (Fig. 3F, n=5/7) with respect to the control side (Fig. 3C; n=7).

Migratory neural crest cells are a mixture of different population subtypes identified by differential gene expression (Del Barrio and Nieto, 2004; Krispin et al., 2010). To determine if the NCCs delaminating prematurely upon FGF signaling blockage were specifically those expressing *Sox10*, we examined the effects on a whole cohort of NCC markers. After 18-20 hours of dn-FGFRI expression using as reporter a nuclear EGFP (pCIG-FGFRdn), there was an increased in the migratory NCC subpopulations expressing Pax7 (Fig. 3G; n=10/11; 170±29% with respect to control side; Fig. S4G), Sox5 (Fig. S4D,G; n=13/13; 159±24 % increase), AP2 (Fig. S4E,G; n=7/7; 149±13 % increase), Pax3, *Snail2* and *FoxD3* (data not shown; n=9/9; 4/4 and 5/6, respectively) transcription factors in comparison to control side and to pCIG electroporated embryos (Fig. 3D and Fig. S4E-G; n=8; 8, 6, 6, 3 and 8 respectively).

Remarkably, not all the prematurely migrating NCCs were electroporated GFP^+ cells (Fig. S4D). To determine if there was a non cell-autonomous effect upon FGFR blockage, we analyzed the number of $Sox5^+$ migratory cells that were either GFP^+ or GFP^- in relation to the number of migratory $Sox5^+$ cells in the control non electroporated side (as a way of normalization to reduce axial level variations; Fig. S4H). The relative number of double GFP^+, $Sox5^+$ migratory cells with respect to the

total $Sox5^+$ migratory cells in the control side was significantly increased in FGFRdn embryos respect to control pCIG (68± 28% in FGFRdn and 42± 15% in pCIG; Fig. S4H). Interestingly, the relative number of GFP^-, $Sox5^+$ cells was also significantly increased in FGFRdn embryos with respect to control pCIG (192± 61% in FGFRdn and 65± 7% in pCIG; Fig. S4H). All these data suggest that the premature migration of the FGFRdn-GFP electroporated cells was also promoting the exit of adjacent non-GFP NCCs and thus, the effect on FGFR blockage would be in part non-cell-autonomous on NCCs. Moreover, while NCC markers such as *Sox10*, *Snail2* and Sox5 were prematurely expressed (Fig. 3B and data not shown) and more ventrally expressed (Sox10; Fig. 3B'), expression of dorsal markers such as *Pax7* and *Msx1* was not affected in the neural tube at epithelial somite levels (Fig. 3G and H; n=6 and 10, respectively). In conclusion, blocking FGF signaling in the neural tube adjacent to PSM promotes premature NCC specification and emigration from the neural tube.

To determine if ectopically maintaining the FGF could prevent neural crest cells from delaminating, we placed FGF8/4 soaked beads in contact with HH11-12 dorsal neural tube at a level where NCCs have already been specified, but before they start *Sox10* expression. As expected, 18 hours later FGF4/8 promoted expression of its direct target *Sprouty2* in the adjacent neuroepithelial cells in HH15-17 embryos [Fig. 4A-B; n=3 (FGF8); 4 (FGF4); Minowada et al., 1999). In contrast to NCCs exposed to control BSA (Fig. 4C,E; n=3 and 5, respectively), the presence of FGF4/8 drastically reduced *Sox10* [Fig. 4D; n=3/4 (FGF4) and 3 (FGF8)] and *Snail2* [Fig. 4F; n=4 (FGF4) and 6 (FGF8)] expression and blocked NCCs emigration. These data indicate that FGF maintains dorsal neural tube cells uncommitted with respect to neural crest fate and that FGF signaling decrease is necessary to promote NCC specification and subsequent migration from the neural tube.

The timing of NCC emigration confers different migratory behavior

In the trunk region of avian embryos, NCCs migrate in a stereotypical manner, leading to a general ventral to dorsal order of derivative colonization beginning with sympathetic ganglia, and finally melanocytes (Le Douarin and Kalcheim, 1999). The final localization of crest cells can be predicted from their relative ventrodorsal position within the premigratory domain or by their time of emigration (Krispin et al., 2010; Henion and Weston, 1997). However, it is also possible that distinct properties of the differentiated mesodermal cells that the NCCs encounter during migration influence their trajectories (Harris and Erickson, 2007).

In order to determine if the NCCs prematurely forced to delaminate upon blockage of FGF signaling had alterations in their migratory behavior, we followed early NCC migration using wide-field real time microscopy of trunk dorsal neural tube in slice culture (Wilcock et al., 2007; Ahlstrom and Erickson, 2009). We used electroporation of H2B-RFP (nucleus) and EGFP-GPI (cell membrane) expressing vectors into stage HH10 chick embryos, to follow individual cells (Fig. 5A,C). Using Metamorph software, we first compared the behavior of the migratory NCCs during the initiation or "first wave" of migration at the level of dissociating somites (somites V-XII) in control EGFP-GPI embryos (Fig. 5A,B,G, Fig. 5video1) in relation to dn-FGFRI-EYFP electroporated NCCs that started prematurely migrating adjacent to epithelial somites (somites I-IV; Fig. 5J; Fig. 5video3). We observed similar speed of migration (16.2±1.8 μm/hr respect to 12.4±1 μm/hr; Fig. 5E) and similar migration straightness (distance covered/length of the trajectory; 0.28±0.07 respect to 0.15±0.4; Fig. 5F) of the two spatially different located populations. These results indicate that the prematurely migrating NCCs, upon FGF signaling blockage, at epithelial somite levels

have a similar behavior to the "first wave" of migrating control NCCs facing dissociating somites.

Conversely, we next analyzed the behavior of dn-FGFRI-EYFP expressing NCCs (Fig. 5C,D,H; Fig5video2) that were migrating next to dissociating somites, in comparison to the first migrating NCCs expressing EGFP-GPI (Fig. 5A). The average speed of the migratory NCCs upon 12 hours period was higher in NCCs expressing dn-FGFRI-EYFP (20.2±1.9 μm/hr; Fig. 5E) with respect to control NCCs (12.4±1 μm/hr; Fig. 5B, E). Moreover, tracking NCCs trajectories revealed that most dn-FGFRI expressing NCCs showed a straight trajectory (Fig. 5H) contrary to control NCCs that exhibited tortuous trajectories and forward and backward movements (Fig. 5F,G; straightness factor of 0.39±0.1 respect to 0.15±0.03). This higher speed and straightness of the more advanced delaminating NCCs expressing dn-FGFRI-EYFP could be a property of a more mature late migrating NCC population, in spite of both control and experimental cells facing the same somitic context. In summary, this analysis reveals distinct migratory properties according to the time of exiting the neural tube.

RA signaling is required to control the timing of NCC emigration

It has been shown that somites are required for the control of the onset of NCC emigration (Sela-Donenfeld and Kalcheim, 2000). However, the molecular nature of those signals emanating from the somites remains unknown. RA signaling is highly active in the neural tube at somitic levels, as revealed by *in vivo* reporter activity driven by RA response elements (RARE) in mouse embryos (Rossant et al., 1991) and by the expression of a read-out of RA signaling, *RARβ (*the RARE promoter elements of which were used in the RARE-LacZ mouse) in chicken embryos (Olivera-Martinez and Storey, 2007). Moreover, the opposing gradients of FGF and RA pathways operate in

concert as a switch that controls progressive neural and limb development (Diez del Corral and Storey, 2004)

To test if RA could be involved in the control of NCC emigration in concert with FGF signaling, we carried out neural tube electroporation of a truncated version of the human α retinoic acid receptor (RAR α) that acts as a dominant negative form for the three RAR receptors (RARdn-IRES-GFP; Novitch el al., 2003). As expected, blocking RAR signaling at HH12-13 decreased the expression of *Pax6* in neural precursors 24 hours post electroporation (Fig. S5; Novitch et al., 2003). In HH12-13 embryos, in which RA signaling was blocked where NCC emigration is starting, the number of cells expressing *Sox10* was reduced and there was a dramatic delay in the emigration of *Sox10*$^{+}$ NCCs (Fig. 6C, n=5/5), in comparison to the pCIG electroporated cells (Fig. 6A, n=5/5). However, more caudally, the initiation of the expression of *Snail2* and *FoxD3*, early markers of NCC specification, was not affected (Fig. 6F; n= 5; Fig. S5 n=6) in comparison with control pCIG electroporated embryos (Fig. 6E; n=3, 8, respectively) indicating that RA is required to establish the onset of NCC emigration independently of NCC specification.

Nevertheless, in HH11-13 embryos electroporated at the level of ongoing NCC migration (somites V-X), RA signaling blockage did not affect the EMT of *Sox10* expressing NCCs compared (Fig. 6B;n= 4) to the control (Fig. 6A; n=6). Similarly, blocking RA signaling did not alter the EMT of AP2^{+} NCCs in comparison to control (Fig. S5; n=6). These data indicate that RA signaling is required to establish the onset but not the maintenance of NCC emigration.

To determine if RA signaling was not only necessary but sufficient to control NCC emigration, we used a constitutively active form of the retinoic acid receptor α fused to the transcriptional activator domain of VP16 (VP16-RAR; Novitch et al.2003). This

construct activates RA target genes in a ligand-independent manner (Castro et al., 1999). VP16-RAR electroporated neuroepithelial cells at the rostral PSM level delaminated prematurely from the dorsal neural tube in comparison with control embryos, as assessed by *Sox10* expression (Fig. 6D; n=5/7; control n=6). Moreover, the initiation of *Snail2* or *FoxD3* expression in caudal neural tube was not affected (Fig. 6G; n=4; and 7 respectively; control n=5 and 8, respectively). In summary, RA signaling is both necessary and sufficient to set the right timing for NCC emigration.

Retinoid signaling is required for very early neural crest specification

Our results have shown that RA signaling is not required for NCC specification during neural tube elongation. However, in *Raldh2* mutants the expression of early NCC markers is severely downregulated (Ribes et al, 2009). To determine if that was exclusive of mammalian embryos we analyzed expression of neural crest markers in vitamin A-deficient (VAD) quails, which represent a retinoid-deficient state (Maden et al., 1996). In normal quails, *Snail2* expression starts in the dorsal neural tube next to mid-PSM (Fig. 7 A) while is strongly reduced in VAD NCCs (Fig. 7B). Similarly, in RA deficient conditions *Sox9* expression is clearly absent from the dorsal neural tube at the rostral PSM level (Fig. 7D) in comparison with normal embryos (Fig. 7C). To determine how early RA signaling is required for NCC specification *Pax7* expression, a key mediator of neural plate border specification (Basch et al., 2006), was examined. In, VAD embryos *Pax7* is absent at the neural plate border (Fig. 7F) in comparison with normal quails (Fig. 7E). As the VAD quails represent an early RA deficient state, these findings suggest that RA signaling is required for the earliest steps in dorsal and NCC specification during gastrulation, before the RA activity is restricted to the neural tube adjacent to rostral PSM, and not for NCC specification during neural tube elongation.

FGF maintains *Noggin* gradient in the caudal neural tube

It has been reported that a R-C gradient of BMP signaling in the dorsal neural tube, generated by the graded expression of the BMP antagonist *Noggin*, is involved in determining the onset of NCC emigration (Sela-Donenfeld and Kalcheim, 1999). As the *Noggin* gradient is controlled by unknown signals coming from the mesoderm (Sela-Donenfeld and Kalcheim, 2000), we tested if FGF and/or RA could be those signals. First we determined whether FGF signaling was required for *Noggin* expression, as both coincide in the caudal neural tube (Fig. 1L, 8A). In cultured embryos at stage HH10-11, briefly exposed (4 hours) to the FGFRI inhibitor PD173074, *Noggin* expression in the neural tube was not affected in comparison to control DMSO treated embryos (Fig. 8A,B; n=8 and 8, respectively). Similarly, after 18-20 hours of dnFGFRI electroporation *Noggin* and *BMP4* expression were not altered in relation to control GFP cells (Fig.8C,D; n=7 and 4, respectively; data not shown). However, exposing neural tube explants at the rostral PSM level to high doses of FGF4 promoted *Noggin* expression after just 4 hours in culture (Fig. 8L, n=10), relative to BSA control explants (Fig. 8K, n=9), while *Snail2* expression (Fig. 8G,H; control n=4; FGF4 n=3) was downregulated, as previously observed with FGF4/8-beads (Fig. 4F). *Sox10* expression was also downregulated after 8 hours, time required for *Sox10* mRNA to be detected in control explants (Fig. 8I,J; control n=12; FGF4 n=9). As a control, *Pax6* was downregulated by FGF4 in neural tube explants at somitic level (Fig. 8E, F; FGF4 n=16, control n=15; Bertrand et al., 2000). Thus, the caudo-rostral FGF signaling gradient is sufficient but not necessary for *Noggin* expression.

To test if RA was the signal responsible for repression of *Noggin* transcription, RARdn was electroporated in NCCs adjacent to rostral PSM. RARdn-electroporated

NCCs exhibited similar levels of *Noggin* expression (Fig. 8 D; n=4) to that of control (Fig. 8 C; n=3). Similarly, in trunk explants at the caudal PSM level exposed for 4 hours to the RAR agonist TTNPB, which induced high levels of *Pax6* (Fig. 8K, L; TTNPB n=10, control n=9; Novitch et al., 2003), *Noggin* expression was similar to that in control DMSO treated explants, 4 and 8 hours after culture (Fig. 8M, N; control-4h n=10 TTNPB-4h, n=12; control-8h n=4 TTNPB-8h, n=4).

In summary, these results indicate that RA does not control NCC emigration through the downregulation of *Noggin* gradient. Moreover, FGF signaling is sufficient but not necessary for *Noggin* expression, suggesting that the decrease in FGF signaling is required for *Noggin* downregulation at somitic levels.

FGF and RA regulate NCC emigration in part through the control of *Wnt1* expression

It has been reported that Wnt ligands are necessary to control *Snail2* expression in NCCs *in vivo* and are sufficient to induce NCCs by *in vitro* assays (García-Castro et al., 2002). Moreover, blocking canonical Wnt signaling prevents NCC emigration (Burstyn–Cohen et al., 2004). However, apart from the control by BMP signaling (Burstyn–Cohen et al., 2004), the regulation of the Wnt pathway has not been extensively analyzed in the NCC during axial elongation. We looked to determine if at NCC emigration FGF and RA signaling could be acting through the modulation of *Wnt1*.

In cultured embryos at stage HH12-14 briefly treated (4 hours) with the FGFRI inhibitor PD173074, the R-C gradient of *Wnt1* expression was prematurely initiated at more caudal levels (Fig. 9B; n=4/7) in comparison with control DMSO treated embryos (Fig. 9A, n=10). Conversely, exposing neural tube explants from rostral PSM levels to

FGF4 for 4 hours in culture inhibited *Wnt1* expression (Fig. 9C, D; FGF4 n=6, BSA n=8; described for longer incubation times in Olivera-Martínez et al., 2007). In conclusion, FGF signaling levels control the initiation of *Wnt1* expression in the dorsal neural tube.

RA signaling activation in the neural tube adjacent to somitic level coincides with the initiation of *Wnt1* expression (Fig. 1K, 9A). To determine if RA signaling was required for the control of *Wnt1* we examined HH10-11 VAD quail embryos (Fig. 9 G, H). Strikingly, in VAD embryos expression of *Wnt1* and *Wnt3a* (Fig. 9 I, J; at older stages in Wilson et al, 2004) was strongly reduced, particularly at the spinal cord level.in comparison with normal quail embryos. As this could be due to the early NCC specification effect mentioned above, we performed trunk explant experiments in chick embryos, where the NCCs have already been specified. Thus, in trunk explants at the rostral half PSM level *Wnt1* expression was enhanced and caudally expanded after 4 hours exposure to the RAR agonist TTNPB, in comparison to DMSO treated explants (Fig. 9E, F; n=4 and 4, respectively). However, this effect on *Wnt1* expression was not observed in trunk explants at caudal PSM level exposed to TTNPB for 4 or 8 hours in culture (data not shown; DMSO-4h n=6 TTNPB-4h, n=6; DMSO-8h n=4 TTNPB-4h, n=4), where NCCs do not express specifiers as *Snail2* at the time of excision.

In summary, FGF signaling prevents the premature expression of *Wnt1*, while RA signaling triggers the initiation of *Wnt1* expression in the dorsal neural tube only at levels where the NCCs are already specified. Given the short time required for its action in culture, FGF and RA could control the timing of NCC emigration through direct changes in *Wnt1* expression.

Discussion

During embryonic development it is essential to coordinate the formation of adjacent tissues that maintain close functional relationships. In this work, we have now established the mechanism that ensures the correct coordination between the formation of central and peripheral nervous system in the trunk during the extension of the body axis. We have demonstrated that FGF and RA signaling set the correct timing for the crucial step of neural crest cell EMT and emigration, necessary for the distribution of peripheral nervous system progenitors along the body axis.

Our work reinforces the idea that dorsal neuroepithelial progenitors in the caudal neural tube are maintained in an uncommitted state due to the presence of strong FGF/MAPK signaling pathway. Therefore the caudo-rostral gradient of FGF prevents the initiation of the neurogenesis program, the onset of the ventral patterning system (Diez del Corral et al., 2003) and also the onset of trunk NCC specification (data presented here). Thus, in the elongating neural tube, as the dorsal neuroepithelial progenitors are progressively exposed to decreasing FGF signaling levels, they initiate the expression of neural crest specifier genes *Snail2* and *FoxD3*. In our experiments, forcing a reduction in FGF signaling allows neuroepithelial cells to prematurely initiate (just after four hours) the expression of both the early NCC specifier *Snail2* at caudal levels and more rostrally the expression of *Wnt1*(signal required for NCC emigration; García-Castro et al., 2002; Burstyn –Cohen et al., 2004). However, only later on when those prematurely *Snail2* expressing NCCs initiate the expression of *FoxD3*, *Sox5*, and finally *Sox10* (after 14 hours of FGF signaling blockage; Fig. 3) they would prematurely start EMT from the neural tube at mid-rostral PSM levels. Essentially, FGF signaling is primary responsible for the control of the initiation of NCC specification in the trunk, and as a consequence of that, it controls the timing of EMT and emigration.

Furthermore, FGF blockage of NCC emigration is mediated in part by maintaining high levels of *Noggin* and low levels of *Wnt1* in the caudal neural tube (Fig. 10).

Although BMP signaling controls the expression of cytoskeletal components involved in EMT such as *Cadherin6B* (Park and Gumbiner, 2010) and *RhoB* (Liu et al., 1998), altering BMP activity does not change *Snail2* expression and does not affect NCC specification (Sela-Donenfeld and Kalcheim, 1999). Given that most of the NCC specification studies done in *Xenopus* embryos concern the cephalic NCCs, our work shows that FGF pathway is, so far, the only signaling pathway clearly controlling the onset of NCC specification at trunk level. This FGF function could be another example of a general FGF role in controlling the onset of differentiation of all cell types as they are generated at the tail end.

Our study also points out the relevance of controlling *Snail2* expression to initiate NCC specification. Not only is *Snail2* expression ectopically activated just after four hours of FGF signaling blockage, in comparison to *FoxD3* which remained unchanged, but *Snail2* is one of the earliest NCC specifier genes being expressed during trunk NCC formation (this paper Fig. 1) and also during the caudal-most NCC development (caudal vertebrae level) where *Snail2* expression also precedes that of *Sox9* and *FoxD3* (Osorio et al., 2009).The regulation of *Snail* genes expression by FGF seems to be context dependent during development. While *Snail1* is induced by FGF8 in lateral mesoderm (Boettger et al., 1999) and primitive streak (Ciruna and Rossant, 2001) and by FGF3 in bone development (De Frutos et al., 2007), it is repressed by FGF in the somites (Boettger et al., 1999) and *Snail2* is repressed in the dorsal neural tube (this paper). Furthermore, controlling the right levels of FGF signaling is essential to modulate *Snail* genes expression. In *Xenopus* embryos, FGF signaling is involved in cephalic NCC

induction (Monsoro-Burq et al, 2003). However, an excess of FGF signaling inhibits *Snail2* expression and NCC formation (Hong and Saint-Jeannet, 2007).

By contrast to FGF signaling acting at caudal level, RA signaling is operating at somitic levels. Our data demonstrate that, at least during trunk elongation, RA signaling is not required for the control of NCC specification but regulates the timing of NCC emigration. Thus, the onset of *Snail2* expression is not affected by changes in RA signaling, but the onset of emigration of *Sox10*$^{+}$ NCCs cells at the mid–rostral PSM level can be modulated changing RA signaling.

BMP activity regulates emigration of already specified neural crest cells (Sela-Donenfeld and Kalcheim, 1999), through the control of *Wnt1* expression (Burstyn-Cohen et al., 2004). RA activity controls emigration modulating, together with FGF signaling, the onset of *Wnt1* expression in the dorsal neural tube at rostral PSM levels (Fig. 10). Thus, our experiments have established that both FGF and RA signaling act as upstream pathways to the BMP/Noggin-Wnt1 signaling cascade to set the right timing for NCC emigration to keep it in register with somite formation. However, the effect of RA on emigration only occurs at rostral PSM and last formed somites level. More rostrally, inhibiting RA signaling does not affect ongoing emigration, probably because BMP signaling is sufficient to maintain the process (Burstyn-Cohen et al., 2004). Conversely, at most caudal neural tube level changes in FGF or RA signaling are not sufficient to induce premature *Wnt1* expression (Fig. 9), and consequently NCCs cannot delaminate from the most caudal part of the neural tube. This time, the absence of BMP signaling at caudal levels could be responsible for the impossibility of emigration.

The consequences of altering the timing of migration could be crucial for the development of the NCC derivatives. It has recently been shown that the final localization of crest cells can be predicted by their time of emigration (Krispin et al.,

2010).. Here, we have demonstrated that the different NCC populations do differ in their migratory behavior, as the first migratory cells (including those prematurely forced to migrate in our experiments; Fig. 5) move at lower speed and follow more tortuous paths than later migrating NCCs. It remains to be seen if changes in migratory behavior adopted in an inappropriate context (non differentiated somites) will have consequences in the final differentiation of the NCCs.

In summary, our data show that there is a limited time window during which the onset of the NCC emigration can be modulated, once those cells have acquired the expression of the essential gene network of the NCC specification program. That window coincides with the region where FGF and RA gradients collide and it is required to keep the emergence of peripheral nervous system progenitors in register with the progressive programs of spinal cord neurogenesis and somites development during trunk axial elongation.

Materials and methods

In situ hybridization

Chickens eggs were incubated at 38ºC in an atmosphere of 70% humidity. Embryos were staged according to Hamburger and Hamilton (HH; Hamburger and Hamilton, 1951). Embryos were fixed overnight at 4ºC with 4% paraformaldehyde in PBS, rinsed and processed for whole-mount *in situ* hybridization. Briefly, embryos were treated with 1% H2O2 and 10 µg/ml proteinase K, refixed in 4% paraformaldehyde and then hybridized overnight at 57IC in a 5XSSC buffer containing 50% formamide with digoxigenin-or fluorescein-labelled riboprobes, as described previously (Martínez-Morales et al., 2010). The chick *Pax7, Snail2, Sox5 Sox10, FoxD3, Sox9, Sax1, Pax6, Raldh2, FGF8*, *Sprouty2, Noggin* and *Wnt1* riboprobes have been described elsewhere (Perez-Alcala et al., 2004; Cheung and Briscoe, 2003; Diez del Corral et al., 2003; Burstyn-Cohen et al., 2004). Chicken *VE-cadherin* was cloned using primers 5' TCC TTC ATT CCT CTC ATC CTG TG 3' (forward) and 5' TGC CGC TCC AAA ACC TTA CTT CC 3' (reverse), following recommendations from C. A. Roselló (M. Torres laboratory). Four to fifteen embryos were analyzed for each experimental condition. The probe hybridization was detected with alkaline phosphatase–coupled with either anti-digoxigenin Fab fragments (Roche) or anti-fluorescein Fab fragment (Roche) and developed with NBT/BCIP or INT/BCIP. Hybridized embryos were postfixed in 4% paraformaldehyde, vibratome sectioned and immunostaining was performed as described above to visualize GFP^+ electroporated cells.

Embryo and explant culture

Chicken embryos at Hamburguer and Hamilton stages HH11-12 were cultured onto collagen beds [prepared as a mixture containing 2.9 mg/ml collagen rat tail (BD

Biosciences), 1x L15 (Invitrogen) and 0.6% NaHCO3 to achieve proper polymerization] covered with Opti-Mem® Medium(Invitrogen) supplemented with 5% FBS serum, 2mM glutamine and 50µg/ml gentamicin. Inhibitors were added to the culture medium (100 µM SU5402, 100 µM PD184352, 10 µM PD173074, 100 µM LY294002, 10 µM KRN633 or DMSO vehicle). Embryos were cultured 4 h at 37ºC, 5% CO_2 before fixation in 4% (w/v) paraformaldehyde in PBS overnight at 4ºC. For FGF treatment chicken embryos stages HH10-11 were put in EC culture (Chapman et al., 2001) before grafted with heparin –coated beads soaked in PBS or FGF8b (50µg/ml) or FGF4 (50 or 500 µg/ml; an inducer of MAPK like FGF8; Diez del Corral et al., 2002;Sigma). Both FGF4 and FGF8 provoked a decrease in the expression of *Snail2* and *Sox10*, but, obviously, with the highest concentration the effect was more extensive affecting a larger area of premigratory neural crest cells. Following incubation at 38ºC for 18-20 hours, embryos were either processed for whole mount *in situ* hybridization or dissected to obtain explants for quantitative RT-PCR. Retinoid –deficient quail embryos were a gift of Emily Gale and Malcolm Maden (King´s College London, UK), and normal and deficient quail embryos were fixed and processed together for *in situ* hybridization (see Diez del Corral et al., 2003).

Explants were dissected from HH9-13 embryos treated with trypsin to separate the neural tissue from the mesoderm when necessary (Diez del Corral et al., 2002). Explants were cultured in collagen beds and cultured covered in Opti-Mem® medium as above containing either BSA or 360ng/ml FGF4 (both supplemented with 0.1ng/µl heparin) or containing KRN633 (Calbiochem,10 µM); DMSO (0.1%) or TTNPB (Calbiochem, 10µM).

Western blot analysis

Western blot analysis was performed by an established method. 20-µg protein samples of each total cell extract were separated by 12% SDS-PAGE, transferred to a PVDF Immobilon-P Membrane (Milipore), and probed with antibodies anti- phospho-AKT (rabbit IgG, Cell Signaling); anti-total-AKT1/2 (H136; Santa Cruz); anti-phospho-Erk1/2(Thr202/Tyr204; Cell Signaling) and anti-total-Erk1/2 (Zymed, San Francisco, CA). Signals were detected with HRP-conjugated secondary antibodies (Jackson ImmunoResearch Laboratories, Inc.) using an ECL Advance Western Blotting Detection Kit (GE Healthcare). Quantitative analysis was obtained by densitometry (GS-800 Densitometer). Results shown are representative of three or more experiments.

Quantitative real-time PCR (qRT-PCR)

Explants of neural tube together with notochord at caudal presomitic mesoderm levels were dissected from embryos cultured for 4h in the presence of DMSO or PD173074 and total RNA isolated using the Quickgene RNA tissue kit SII (Fujifilm Global). cDNA was synthesised with Superscript III DNA polymerase (Invitrogen) and random primers (Invitrogen). Real-time PCR was carried out in an Applied 7500 PCR System using Power SYBR Green Master Mix (Applied Biosystems) and sequence specific primers (Sigma). Sequences of *Snail2* primers are: 5'AGCCAAACTACAGCGAACTG 3' (forward) and 5′ TGATAGGGACTGGGTAGCTTTC 3' (reverse) and sequences for *Sprouty2* primers are: 5' ATCATCTTCAGGGCCAGTTG 3′ (forward) and 5′ TGCTCCCAAGTCTTCTTTGC-¡3′ (reverse). 18S rRNA was used as a reference gene. *Sprouty2* levels were determined using the Standard curve method while *Snail2* levels were determined by the comparative CT method following Applied Biosystems recommendations based on validation experiments assessing whether efficiencies of target and reference are approximately equal. Three lots of four to twelve explants

generated in three independent experiments were used. Each of these samples was retrotranscribed and the product was used as template for each pair of primers in a triplicate wells PCR reactions and PCR procedure was performed twice.

Constructs

Truncated chick FGF-Receptor1c (aa 1-425) fused to EYFP in a Clontech vector (pEYFP-N1) to generate dnFGFR1-EYFP was kindly provided by C. Weijer (Yang et al., 2002) and was also inserted into pCAGGS-IRES-nuclearEGFP (pCIG; Niwa et al., 1991) to generate pCIG-FGFRdn. The pCAGGS vector containing a membrane tagged EGFP-GPI was used as a control. cDNAs encoding human retinoic acid receptor α truncation mutant 403 (RAR403; Damm et al., 1993) and a VP16-retinoic acid receptor α fusion (Castro et al., 1999) cloned into pCIG were kindly provided by B. Novitch (Novitch et al., 2003). In this case, pCIG was used as control vector.

Chick in ovo electroporation

Chick embryos were electroporated with Qiagen purified plasmid DNA at 1-2 ug/ul in PBS with Fast Green (50 ng/ml), as described previously (Martínez-Morales et al., 2010). Briefly, plasmid DNA was injected in the lumen of HH10-12 neural tubes, electrodes were placed on either side of the neural tube and a train of electric pulses (5 pulses, 14 volts, 50 msec) was applied using an electroporator (Intracel TSS20). Eggs were further incubated for 24 to 48 hours and they were assayed for EGFP expression in the neural tube. Subsequently, the embryos were fixed and processed for immunohistochemistry or *in situ* hybridization.

Immunohistochemistry

Embryos were fixed for 2-4 hours at 4ºC with 4% paraformaldehyde in PBS, and they were immersed in 30% sucrose solution, embedded in OCT and sectioned on a Leica cryostat. Alternatively, embryos were embedded in agarose/sacarose (5%/10%) and they were sectioned in a Leica vibratome (VT1000S). For immunohystochemistry, 10 μm cryostat or 40 μm vibratome agarose sections were permeabilised with 0.5% Triton X-100, blocked with 10% FBS and incubated overnight at 4°C with the primary antibody. After washing, the cryostat sections were incubated for 1 hour with secondary antibodies. Primary antibodies against the following proteins were used: Sox5 (Pérez-Alcalá et al., 2004); green fluorescence protein (GFP; Molecular Probes), Laminin (Sigma). Monoclonal antibodies against Pax7, Msx1 (4G1), Pax6, AP2 (3B5), Pax3 and Snail (62.1E6),were all obtained from the Developmental Studies Hybridoma Bank (developed under the auspices of NICHD and maintained by the University of Iowa). Alexa 488- and Cy3-conjugated anti-mouse or anti-rabbit secondary antibodies (Molecular Probes) were used for detection and after staining, the sections were mounted in Citifluor plus Bisbenzimide and photograph using a Leica confocal microscope.

Real time imaging

Embryos at stage HH 10-11 were electroporated with a concentration of 0.2 μg/μl H2B-RFP either with 1μg/μl GFP-GPI or dnFGFR1-EYFP. Embryos were incubated at 38°C for 18 hours (for imaging at HH15-16 stages). Slices of ~150 μm were taken from the trunk on stage HH16-18 chicken embryos (Wilcock et al. 2007) at the axial level of caudal, epithelial (somite I-IV) or rostral dissociated (somite V-XII) somites. Explants were cultured as described by Wilcock et al. 2007. Briefly, slices of ~150 μm were taken with a microknife, embedded in rat tail collagen type I in coverslip-based petri

dishes (WillCo-dish glass-bottom dish, Intracel, Royston, UK; GWst-3522, coated with poly-L-lysine, Sigma) and cultured in Neurobasal medium, without phenol red (Gibco), supplemented with B-27 to a final 1X concentration with L-glutamine and gentomycin maintained at 37°C with 5% CO2/air for ~4 hours before imaging. Slices were imaged on a DeltaVision Core microscope workstation (Applied Precision, LLC, Issaquah, WA; Wilcock et al. 2007). Care was taken to image slices at least 20 μm past the cut surface, and only where the ectoderm was intact over the dorsal neural tube. Images were captured using a 40X1.30 NA objective lens with a Xenon lamp. Optical sections (exposure time=50 milliseconds, 512x512 pixels, bin=2x2) were spaced by 2 μm and imaged at 7-minute intervals for up to 24 hours. The images obtained were deconvolved and projected using DeltaVision software (softWoRx®). Metamorph ® software was used to analyze the neural crest trajectory and the speed of migration. For each experimental condition, 10 cells were analyzed during a period of 4-12 hours from at least four embryos.

Image acquisition and processing.

Transmited light images where acquired in a Nikon Eclipse 80i upright microscope with Nikon Digital Sight D5-U1 or DXM1200F cameras using Nikon Act-1 or Act-2u software. Whole embryos and explants were mounted in 50%PBS/50% glycerol and photographed with x10/0.3 Plan Fluor, 20x/0.75 Plan Apo or 20x/0.5 Plan Fluor objectives. Vibratome sections where mounted in 50%PBS/50% glycerol and photographed with a 40x/0.75 Plan Fluor objective. Fluorescence labeled sections were mounted in Citifluor plus Bisbenzimide and confocal images where taken using a Leica TCS SP5 system and 40x/1.40 oil UV corrected objective. Fluorochromes used were Bisbenzimide (Molecular Probes), Alexa Fluor 488 (Molecular Probes) and Cy3

(Jackson Immunoresearch). Images were assembled and corrected contrast and brightness using Adobe Photoshop CS3.

Supplemental Materials

Supplementary Figure 1. Analysis of NCC specification and emigration upon FGFR blockage using the PD173074 inhibitor.

Supplementary Figure 2. VEGFR activity inhibition does not alter *Snail2* expression in the neural tube

Supplementary Figure 3. Blockage of FGF signaling pathway promotes premature *Pax6* expression and prevents *Sprouty2* expression in the neural tube.

Supplementary Figure 4. Blockage of FGF signaling pathway promotes NCCs premature emigration of several populations.

Supplementary Figure 5. RA signaling is not required to maintain NCC emigration. RA signaling does not control the onset of FoxD3 expression in the neural tube

Fig5video 1. Movie showing the migration of NCCs electroporated with H2B-RFP (red) and with control EGFP-GPI (green) at the level of differentiating somites .

Fig5video 2. Movie showing the migration of NCCs electroporated with H2B-RFP (red) and with dnFGFR1-EYFP (green) at the level of differentiating somites.

Fig5video 3. Movie showing the migration of NCCs electroporated with H2B-RFP (red) and with dnFGFR1-EYFP (green) at the level of epithelial somites.

Acknowledgements

We thank P. Bovolenta for her support and suggestions along the project; M.A. Nieto for useful comments on the manuscript; A. Arias, I. Ocaña and V. Barbero for excellent technical assistance and E. Cisneros for advice on qRT-PCR.. VAD quails were kindly provided by M. Maden and E. Gale (MRC Centre for Developmental Neurobiology, KCL). B. Novitch, C. Weijer, H. Nakamura for cDNAs and M. Torres for primers and reagents. This work was funded by the Spanish MCINN grants to A.V.M. (BFU2005-00762 and BFU2008-02963) and to R.D.C. (BFU2005-02972). A.V.M. was supported by the RyC Programme, P.L.M by a FPU fellowship, K.G.S and I.O-M were funded by MRC grant G0600234, R.A.D by Wellcome Trust grant to KGS 083611/Z/07/Z.

Abbreviations List

AKT, protein kinase B (also abbreviated PKB); BMP, bone morphogenetic protein; EMT, epithelial-mesenchymal transition; ERK, extracellular signal-regulated kinase; HH, Hamburguer and Hamilton; MEK, mitogen-activated protein kinase kinase; NCC, neural crest cells; PSM, presomitic mesoderm; PI3K, phosphatidyl-inositol-3-phosphate; RA, retinoic acid; R-C, rostro-caudal.

References

Ahlstrom, J.D., and C.A. Erickson. 2009. The neural crest epithelial-mesenchymal transition in 4D: a 'tail' of multiple non-obligatory cellular mechanisms. *Development*. 136:1801-12.

Barrallo-Gimeno, A., J. Holzschuh, W. Driever, and E.W. Knapik. 2004. Neural crest survival and differentiation in zebrafish depends on mont blanc/tfap2a gene function. *Development*. 131:1463-77.

Basch, M.L., M. Bronner-Fraser, and M.I. Garcia-Castro. 2006. Specification of the neural crest occurs during gastrulation and requires Pax7. *Nature*. 441:218-22.

Bertrand, N., F. Medevielle, and F. Pituello. 2000. FGF signaling controls the timing of Pax6 activation in the neural tube. *Development*. 127:4837-43.

Boettger, T., L. Wittler, and M. Kessel. 1999. FGF8 functions in the specification of the right body side of the chick. *Curr Biol*. 9:277-80.

Brewster, R., J. Lee, and A. Ruiz i Altaba. 1998. Gli/Zic factors pattern the neural plate by defining domains of cell differentiation. *Nature*. 393:579-83.

Bronner-Fraser, M. 1986. Guidance of neural crest migration. Latex beads as probes of surface-substratum interactions. *Dev Biol (N Y 1985)*. 3:301-37.

Burstyn-Cohen, T., J. Stanleigh, D. Sela-Donenfeld, and C. Kalcheim. 2004. Canonical Wnt activity regulates trunk neural crest delamination linking BMP/noggin signaling with G1/S transition. *Development*. 131:5327-39.

Castro, D.S., M. Arvidsson, M. Bondesson Bolin, and T. Perlmann. 1999. Activity of the Nurr1 carboxyl-terminal domain depends on cell type and integrity of the activation function 2. *J Biol Chem*. 274:37483-90.

Casanova, J.C., V. Uribe, C. Badia-Careaga, G. Giovinazzo, M. Torres, and J.J. Sanz-Ezquerro. 2011. Apical ectodermal ridge morphogenesis in limb development is controlled by Arid3b-mediated regulation of cell movements. *Development*. 138:1195-205.

Cheung, M., and J. Briscoe. 2003. Neural crest development is regulated by the transcription factor Sox9. *Development*. 130:5681-93.

Ciruna, B., and J. Rossant. 2001. FGF signaling regulates mesoderm cell fate specification and morphogenetic movement at the primitive streak. *Dev Cell*. 1:37-49.

Damm, K., R.A. Heyman, K. Umesono, and R.M. Evans. 1993. Functional inhibition of retinoic acid response by dominant negative retinoic acid receptor mutants. *Proc Natl Acad Sci U S A*. 90:2989-93.

de Frutos, C.A., S. Vega, M. Manzanares, J.M. Flores, H. Huertas, M.L. Martinez-Frias, and M.A. Nieto. 2007. Snail1 is a transcriptional effector of FGFR3 signaling during chondrogenesis and achondroplasias. *Dev Cell*. 13:872-83.

Del Barrio, M.G., and M.A. Nieto. 2004. Relative expression of Slug, RhoB, and HNK-1 in the cranial neural crest of the early chicken embryo. *Dev Dyn*. 229:136-9.

Diez del Corral, R., D.N. Breitkreuz, and K.G. Storey. 2002. Onset of neuronal differentiation is regulated by paraxial mesoderm and requires attenuation of FGF signaling. *Development*. 129:1681-91.

Diez del Corral, R., I. Olivera-Martinez, A. Goriely, E. Gale, M. Maden, and K. Storey. 2003. Opposing FGF and retinoid pathways control ventral neural pattern, neuronal differentiation, and segmentation during body axis extension. *Neuron*. 40:65-79.

Diez del Corral, R., and K.G. Storey. 2004. Opposing FGF and retinoid pathways: a signaling switch that controls differentiation and patterning onset in the extending vertebrate body axis. *Bioessays*. 26:857-69.

Dottori, M., M.K. Gross, P. Labosky, and M. Goulding. 2001. The winged-helix transcription factor Foxd3 suppresses interneuron differentiation and promotes neural crest cell fate. *Development*. 128:4127-38.

Dubrulle, J., M.J. McGrew, and O. Pourquie. 2001. FGF signaling controls somite boundary position and regulates segmentation clock control of spatiotemporal Hox gene activation. *Cell*. 106:219-32.

Echevarria, D., S. Martinez, S. Marques, V. Lucas-Teixeira, and J.A. Belo. 2005. Mkp3 is a negative feedback modulator of Fgf8 signaling in the mammalian isthmic organizer. *Dev Biol*. 277:114-28.

Garcia-Castro, M.I., C. Marcelle, and M. Bronner-Fraser. 2002. Ectodermal Wnt function as a neural crest inducer. *Science*. 297:848-51.

Goulding, M.D., G. Chalepakis, U. Deutsch, J.R. Erselius, and P. Gruss. 1991. Pax-3, a novel murine DNA binding protein expressed during early neurogenesis. *Embo J*. 10:1135-47.

Harris, M.L., and C.A. Erickson. 2007. Lineage specification in neural crest cell pathfinding. *Dev Dyn*. 236:1-19.

Henion, P.D., and J.A. Weston. 1997. Timing and pattern of cell fate restrictions in the neural crest lineage. *Development*. 124:4351-9.

Hong, C.S., and J.P. Saint-Jeannet. 2007. The activity of Pax3 and Zic1 regulates three distinct cell fates at the neural plate border. *Mol Biol Cell*. 18:2192-202.

Kalcheim, C., and N.M. LeDouarin. 1999. The neural crest. Cambridge University Press, Cambridge, UK.

Kawakami, A., M. Kimura-Kawakami, T. Nomura, and H. Fujisawa. 1997. Distributions of PAX6 and PAX7 proteins suggest their involvement in both early and late phases of chick brain development. *Mech Dev*. 66:119-30.

Khudyakov, J., and M. Bronner-Fraser. 2009. Comprehensive spatiotemporal analysis of early chick neural crest network genes. *Dev Dyn*. 238:716-23.

Krispin, S., E. Nitzan, Y. Kassem, and C. Kalcheim. 2010. Evidence for a dynamic spatiotemporal fate map and early fate restrictions of premigratory avian neural crest. *Development*. 137:585-95.

Kos, R., M.V. Reedy, R.L. Johnson, and C.A. Erickson. 2001. The winged-helix transcription factor FoxD3 is important for establishing the neural crest lineage and repressing melanogenesis in avian embryos. *Development*. 128:1467-79.

Liem, K.F., Jr., G. Tremml, H. Roelink, and T.M. Jessell. 1995. Dorsal differentiation of neural plate cells induced by BMP-mediated signals from epidermal ectoderm. *Cell*. 82:969-79.

Liu, J.P., and T.M. Jessell. 1998. A role for rhoB in the delamination of neural crest cells from the dorsal neural tube. *Development*. 125:5055-67.

Loring, J.F., and C.A. Erickson. 1987. Neural crest cell migratory pathways in the trunk of the chick embryo. *Dev Biol*. 121:220-36.

Lunn, J.S., K.J. Fishwick, P.A. Halley, and K.G. Storey. 2007. A spatial and temporal map of FGF/Erk1/2 activity and response repertoires in the early chick embryo. *Dev Biol*. 302:536-52.

Maden, M., E. Gale, I. Kostetskii, and M. Zile. 1996. Vitamin A-deficient quail embryos have half a hindbrain and other neural defects. *Curr Biol*. 6:417-26.

Martinez-Morales, P.L., A.C. Quiroga, J.A. Barbas, and A.V. Morales. 2010. SOX5 controls cell cycle progression in neural progenitors by interfering with the WNT-beta-catenin pathway. *EMBO Rep*. 11:466-72.

Martins-Green, M., and C.A. Erickson. 1987. Basal lamina is not a barrier to neural crest cell emigration: documentation by TEM and by immunofluorescent and immunogold labelling. *Development*. 101:517-33.

Minowada, G., L.A. Jarvis, C.L. Chi, A. Neubuser, X. Sun, N. Hacohen, M.A. Krasnow, and G.R. Martin. 1999. Vertebrate Sprouty genes are induced by FGF signaling and can cause chondrodysplasia when overexpressed. *Development*. 126:4465-75.

Mohammadi, M., G. McMahon, L. Sun, C. Tang, P. Hirth, B.K. Yeh, S.R. Hubbard, and J. Schlessinger. 1997. Structures of the tyrosine kinase domain of fibroblast growth factor receptor in complex with inhibitors. *Science*. 276:955-60.

Mohammadi, M., S. Froum, J.M. Hamby, M.C. Schroeder, R.L. Panek, G.H. Lu, A.V. Eliseenkova, D. Green, J. Schlessinger, and S.R. Hubbard. 1998. Crystal structure of an angiogenesis inhibitor bound to the FGF receptor tyrosine kinase domain. *Embo J*. 17:5896-904.

Monsoro-Burq, A.H., R.B. Fletcher, and R.M. Harland. 2003. Neural crest induction by paraxial mesoderm in Xenopus embryos requires FGF signals. *Development*. 130:3111-24.

Morales, A.V., J.A. Barbas, and M.A. Nieto. 2005. How to become neural crest: from segregation to delamination. *Semin Cell Dev Biol*. 16:655-62.

Nakamura, K., A. Yamamoto, M. Kamishohara, K. Takahashi, E. Taguchi, T. Miura, K. Kubo, M. Shibuya, and T. Isoe. 2004. KRN633: A selective inhibitor of vascular endothelial growth factor receptor-2 tyrosine kinase that suppresses tumor angiogenesis and growth. *Mol Cancer Ther*. 3:1639-49.

Nakata, K., T. Nagai, J. Aruga, and K. Mikoshiba. 1997. Xenopus Zic3, a primary regulator both in neural and neural crest development. *Proc Natl Acad Sci U S A*. 94:11980-5.

Nieto, M.A., M.G. Sargent, D.G. Wilkinson, and J. Cooke. 1994. Control of cell behavior during vertebrate development by Slug, a zinc finger gene. *Science*. 264:835-9.

Niwa, H., K. Yamamura, and J. Miyazaki. 1991. Efficient selection for high-expression transfectants with a novel eukaryotic vector. *Gene*. 108:193-9.

Novitch, B.G., H. Wichterle, T.M. Jessell, and S. Sockanathan. 2003. A requirement for retinoic acid-mediated transcriptional activation in ventral neural patterning and motor neuron specification. *Neuron*. 40:81-95.

Olivera-Martinez, I., and K.G. Storey. 2007. Wnt signals provide a timing mechanism for the FGF-retinoid differentiation switch during vertebrate body axis extension. *Development*. 134:2125-35.

Osorio, L., M.A. Teillet, and M. Catala. 2009. Role of noggin as an upstream signal in the lack of neuronal derivatives found in the avian caudal-most neural crest. *Development*. 136:1717-26.

Paratore, C., D.E. Goerich, U. Suter, M. Wegner, and L. Sommer. 2001. Survival and glial fate acquisition of neural crest cells are regulated by an interplay between the transcription factor Sox10 and extrinsic combinatorial signaling. *Development*. 128:3949-61.

Park, K.S., and B.M. Gumbiner. 2010. Cadherin 6B induces BMP signaling and de-epithelialization during the epithelial mesenchymal transition of the neural crest. *Development*. 137:2691-701.

Perez-Alcala, S., M.A. Nieto, and J.A. Barbas. 2004. LSox5 regulates RhoB expression in the neural tube and promotes generation of the neural crest. *Development*. 131:4455-65.

Ribes, V., I. Le Roux, M. Rhinn, B. Schuhbaur, and P. Dolle. 2009. Early mouse caudal development relies on crosstalk between retinoic acid, Shh and Fgf signaling pathways. *Development*. 136:665-76.

Ribisi, S., Jr., F.V. Mariani, E. Aamar, T.M. Lamb, D. Frank, and R.M. Harland. 2000. Ras-mediated FGF signaling is required for the formation of posterior but not anterior neural tissue in Xenopus laevis. *Dev Biol*. 227:183-96.

Rickmann, M., J.W. Fawcett, and R.J. Keynes. 1985. The migration of neural crest cells and the growth of motor axons through the rostral half of the chick somite. *J Embryol Exp Morphol*. 90:437-55.

Rossant, J., R. Zirngibl, D. Cado, M. Shago, and V. Giguere. 1991. Expression of a retinoic acid response element-hsplacZ transgene defines specific domains of transcriptional activity during mouse embryogenesis. *Genes Dev*. 5:1333-44.

Saint-Jeannet, J.P., X. He, H.E. Varmus, and I.B. Dawid. 1997. Regulation of dorsal fate in the neuraxis by Wnt-1 and Wnt-3a. *Proc Natl Acad Sci U S A*. 94:13713-8.

Sauka-Spengler, T., and M. Bronner-Fraser. 2008. A gene regulatory network orchestrates neural crest formation. *Nat Rev Mol Cell Biol*. 9:557-68.

Schonwasser, D.C., R.M. Marais, C.J. Marshall, and P.J. Parker. 1998. Activation of the mitogen-activated protein kinase/extracellular signal-regulated kinase pathway by conventional, novel, and atypical protein kinase C isotypes. *Mol Cell Biol*. 18:790-8.

Sela-Donenfeld, D., and C. Kalcheim. 1999. Regulation of the onset of neural crest migration by coordinated activity of BMP4 and Noggin in the dorsal neural tube. *Development*. 126:4749-62.

Sela-Donenfeld, D., and C. Kalcheim. 2000. Inhibition of noggin expression in the dorsal neural tube by somitogenesis: a mechanism for coordinating the timing of neural crest emigration. *Development*. 127:4845-54.

Skaper, S.D., W.J. Kee, L. Facci, G. Macdonald, P. Doherty, and F.S. Walsh. 2000. The FGFR1 inhibitor PD 173074 selectively and potently antagonizes FGF-2 neurotrophic and neurotropic effects. *J Neurochem*. 75:1520-7.

Stavridis, M.P., J.S. Lunn, B.J. Collins, and K.G. Storey. 2007. A discrete period of FGF-induced Erk1/2 signaling is required for vertebrate neural specification. *Development*. 134:2889-94.

Stewart, R.A., B.L. Arduini, S. Berghmans, R.E. George, J.P. Kanki, P.D. Henion, and A.T. Look. 2006. Zebrafish foxd3 is selectively required for neural crest specification, migration and survival. *Dev Biol*. 292:174-88.

Teillet, M.A., C. Kalcheim, and N.M. Le Douarin. 1987. Formation of the dorsal root ganglia in the avian embryo: segmental origin and migratory behavior of neural crest progenitor cells. *Dev Biol*. 120:329-47.

Tosney, K.W. 1978. The early migration of neural crest cells in the trunk region of the avian embryo: an electron microscopic study. *Dev Biol*. 62:317-33.

Villanueva, S., A. Glavic, P. Ruiz, and R. Mayor. 2002. Posteriorization by FGF, Wnt, and retinoic acid is required for neural crest induction. *Dev Biol*. 241:289-301.

Wilcock, A.C., J.R. Swedlow, and K.G. Storey. 2007. Mitotic spindle orientation distinguishes stem cell and terminal modes of neuron production in the early spinal cord. *Development*. 134:1943-54.

Wilson, L., E. Gale, D. Chambers, and M. Maden. 2004. Retinoic acid and the control of dorsoventral patterning in the avian spinal cord. *Dev Biol*. 269:433-46.

Yang, X., D. Dormann, A.E. Munsterberg, and C.J. Weijer. 2002. Cell movement patterns during gastrulation in the chick are controlled by positive and negative chemotaxis mediated by FGF4 and FGF8. *Dev Cell*. 3:425-37.

Figures Legends

Figure 1. **The onset of expression of NCC markers along the R-C axis coincides with FGF8 decline.** (A-K) Gene expression analysis of stages HH10 (A-F, H-K) and HH12 (G) chicken embryos. *Pax7* (A), *Snail2* (B), *Sox9* (C), *Sox5* (D), *Sox10* (E) and *FoxD3* (F,G). Transverse sections at the last formed somite level (A´-G´) or at the onset of gene expression in the dorsal neural tube (A´´-G´´). (H,I) *Snail2* (left in H,I), *Sax1* (right in H) or *Pax6* (right in I) expression in bilaterally dissected embryos. (J-K) Double *in situ* hybridization for *Snail2* (purple), *Raldh2* (red in J), *FGF8* (red in K). (L) Schema of the approximate axial level of different gene expression in relation to NCC development. Black arrowheads point the last formed somite and red arrows the border of gene expression. Scale bars: A (for A-G); 100µm; A' (for A'-G', A''-G'') 50µm; H (for H,I) 200µm, (for J,K) 300µm.

Figure 2. **FGF signaling controls the onset of trunk NCC specification through the MAPK pathway.** Stage HH11-12 embryos cultured 4 hours in the presence of control (DMSO) or inhibitors for FGFRI (SU5402), MAPKK (PD184352) or PI3K (LY294002) and analyzed for *Sprouty2* expression (A-D) and for *Snail2* (E-H). Black arrowheads point the last formed somite. (E'-H') Transverse sections at the level indicated by a bar in the corresponding figure. (I) Western blot analysis from embryos treated with DMSO or the different inhibitors to detect levels of phosphorylated ERK (p-ERK), in comparison with total ERK, and levels of phosphorylated AKT (p-AKT) in comparison to total AKT. Results shown are representative of at least three experiments. Scale bars: A (for A-H); 100µm; A' (for A'-H') 50µm.

Figure 3. **Blockage of FGF signaling pathway promotes NCCs premature emigration.** Stages HH11-13 embryos electroporated on the right neural hemitube with control membrane EGFP (EGFP-GPI), a control nuclear EGFP (pCIG), a dominant negative truncated version of FGFRI fused to EYFP (dnFGFRI-EYFP) or a dnFGFR in pCIG (FGFRdn-pCIG) constructs, as indicated, and analyzed 18-24 hours later. (A-B) *Sox10* expression. Black arrowheads point the last formed somite, brackets to the electroporated area and black arrows to *Sox10* expression in migratory NCCs. (A'-B') Transverse section at the level indicated by a bar in the corresponding figure.. (C-H) Immunostaining in electroporated embryos showing in red Laminin (Lam; C,F), Pax7 (D,G) and Msx1 (E,H) expression. (C'-H') EGFP/EYFP expression in the electroporated hemitube. White arrows point to border of neural tube basal lamina and white arrowheads to excess of migratory neural crest cells. Scale bars: A (for A-B) 50μm; A' (for A'-B') 40μm, C (for C-H) 30 μm.

Figure 4. **Ectopic FGF inhibits NCC specification and emigration.** Stage HH11-12 embryos were exposed to heparin-coated beads either with PBS (A,C,E) or with FGF4 (B,D,F). After 16-18 hours in culture, *in situ* hybridization analysis of *Sprouty*, *Sox10* and *Snail2* expression. (A'-F') Transversal sections through the region where the bead was located. Black arrowheads point the last formed somite and black arrows point ectopic expression in B' and downregulation of expression in D' and F´. Scale bars: A (for A-F) 100μm; A' (for A'-F') 40μm.

Figure 5. **Analysis of migratory behavior in NCCs after FGF signaling blockage.** Chicken embryos at stages HH10-11 electroporated on the right neural hemitube with H2B-RFP (red) and with GFP-GPI or dnFGFR1-EYFP (both green) and analyzed for

imaging 14-16 hours later.. (A,C) Selected frames taken from a control GFP-GPI(A) or a dnFGFR1-EYFP (C) electroporated embryo at the level of differentiating somites (somite V). Blue arrow point to the same cell along the different frames. The trajectories of cells indicated in A and C are reflected in schemes B and D, respectively. (E,F) Quantitative analysis using Metamorph software of the speed (E) and straightness (F) of NCC migration analyzed at the level of differentiated or epithelial somites. Statistical significance was examined by Student´s t test. (**) $p<0.003$, (*) $p<0.04$, n.s. not significant. (G-J) Schematic representation of the trajectories followed by electroporated NCCs either with control EYFP (G,I) or dn-FGFRI-EYFP (H,J) of four representative embryos, at the level of epithelial somites (I,J) or differentiating somites (G,H). Scale bar: A (A,C) 20μm.

Figure 6. **RA signaling is required at neural tube to control the timing of NCC emigration.** Chicken embryos at stages HH11-13 electroporated on the right neural hemitube with control pCX-IRES-GFP construct (pCIG), a dominant negative truncated version of RARα (pCIG-RARdn) or a constitutively active form of the RARα (RAR-VP16) and analyzed 18-24 hours later. *In situ* hybridization of *Sox10* (A-D) and *Snail2* expression (E-G). Black arrowheads point the last formed somites and brackets to the electroporated area.. (A'-G') Transversal section at the level indicated by a bar. Scale bars: A (for A,B,D) 100μm, (for C, E-G) 80μm; A' (for A'- G') 45μm.

Figure 7. **RA signaling is required for early NCC specification.** Comparison of gene expression patterns in the spinal cord in Vitamin A -deficient quails and control stage matched quail embryos. (A,B) *Snail2*, (C,D) *Sox9*, (E,F) *Pax7*. (A'-F') Transverse

sections at the level indicated in A-F. Scale bars: A (for A-D), 100µm; A' (for A'-D') 50µm.

Figure 8. **FGF maintains *Noggin* expression in the caudal neural tube.** (A,B) Stage HH11-12 embryos cultured for 4 hours in the presence of DMSO (control) or the FGFRI inhibitor (PD173074) and analyzed for *Noggin* expression. Black arrowheads point the last formed somites. (A',B') Transversal section of the respective embryos through the level indicated by a bar. (C,D) Transversal sections of embryos at stages HH11-13 electroporated with control pCIG or with pCIG-dnRAR (RARdn) and analyzed 18-24 hours later for *Noggin* expression. (C´,D') EGFP in the electroporated area. (E -P) Neural tube explants at the level of rostral PSM (E-H, K, L) or the entire PSM (I, J) and trunk explants (including neural tube and mesoderm; M-P) at the level of somites (M, N) or caudal PSM (O, P) cultured during 4 hours or 8 hours (only for I, J) in the presence of the indicated medium and analyzed for the expression of the indicated mRNA. Scale bars: A (for A,B) 90µm; A' (for A'-B') 50µm, (for C-D') 35µm; E (for I, J) 50µm, (for E-H, K, L) 100µm, (for M-P) 85 µm.

Figure 9. **Onset of *Wnt1* expression is controlled by both FGF and RA signaling.** (A-B) Stage HH11-12 embryos cultured for 4 hours in the presence of DMSO (control) or FGFRI inhibitor (PD173074) and analyzed for the expression of *Wnt1* Arrows point the onset of expression in the neural tube. (C-F) Explants of neural tube adjacent to rostral PSM (C,D) or whole trunk (including neural tube and mesoderm; E,F) cultured during 4 hours in the presence of PBS-BSA (C) or DMSO (E) as control, FGF8 (D) or the RA agonist TTNPB (F) and analyzed for *Wnt1* expression. (G-J) Comparison of *Wnt1*(G,H) and *Wnt3a* (I,J) expression in Vitamin A-deficient quails(VAD) and control

stage matched quail embryos (WT). (G'-J') Transverse sections at the level indicated in G-J. Black arrowheads point the last formed somites. Scale bars: A (for A, B) 160 μm; C (for C,D) 50μm, (for E, F) 42 μm; G (for G-J) 100μm; G' (for G'-J') 50μm.

Figure10. **Signaling pathways involved in the control of NCC specification and emigration during trunk elongation.** The FGF signaling (pink), acting through the MAPK pathway, prevents the onset of NCC (green) specification in the caudal neural tube and, through the regulation of *Wnt1* onset of expression (pale red) and *Noggin* (orange) expression, controls de initiation of NCC emigration. The RA signaling (blue) controls the initiation of NCC emigration by modulating NCC genes (dashed arrow) or by controlling the onset of *Wnt1* expression. BMP signaling gradient (green) promotes the onset and maintenance of NCC emigration through the control of *Wnt1* expression (grey lines; data from Burstyn-Cohen et al., 2004).

Martínez-Morales et al. Figure 1

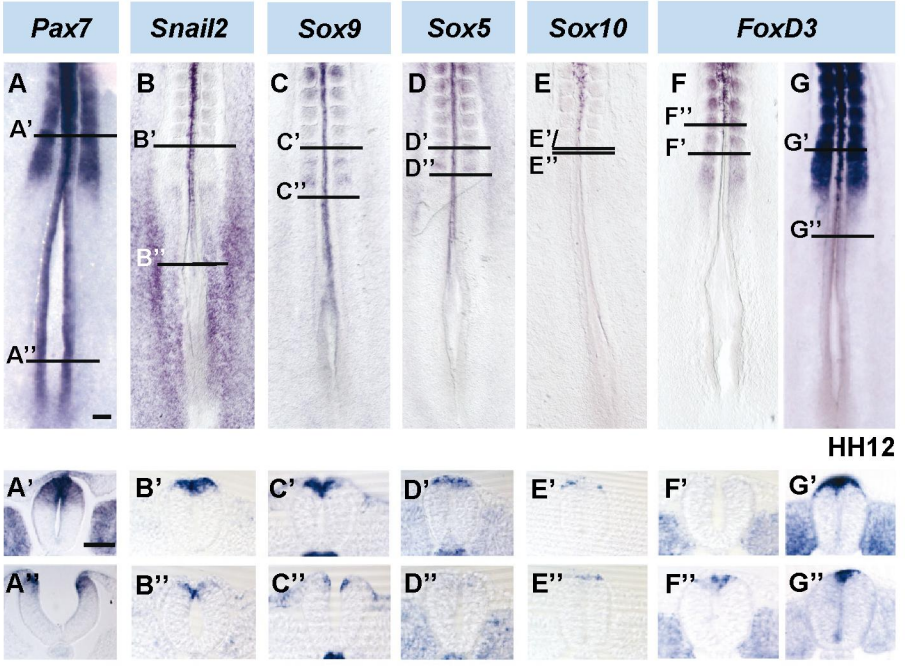

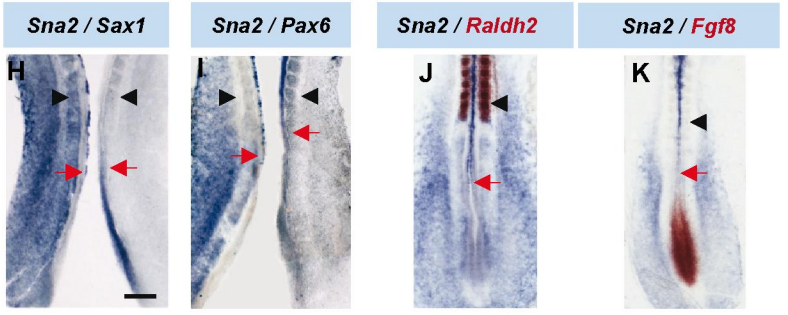

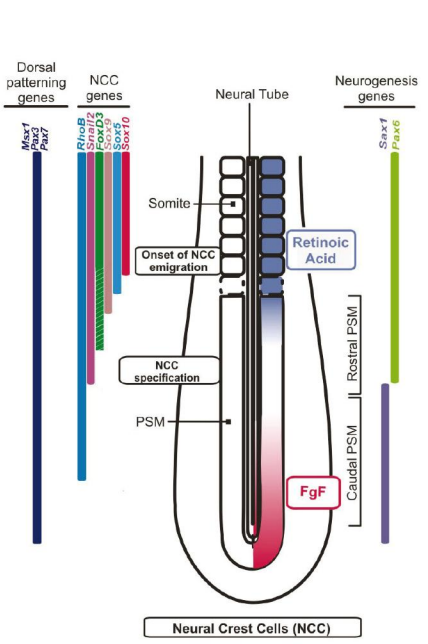

Martínez-Morales et al. Figure 2

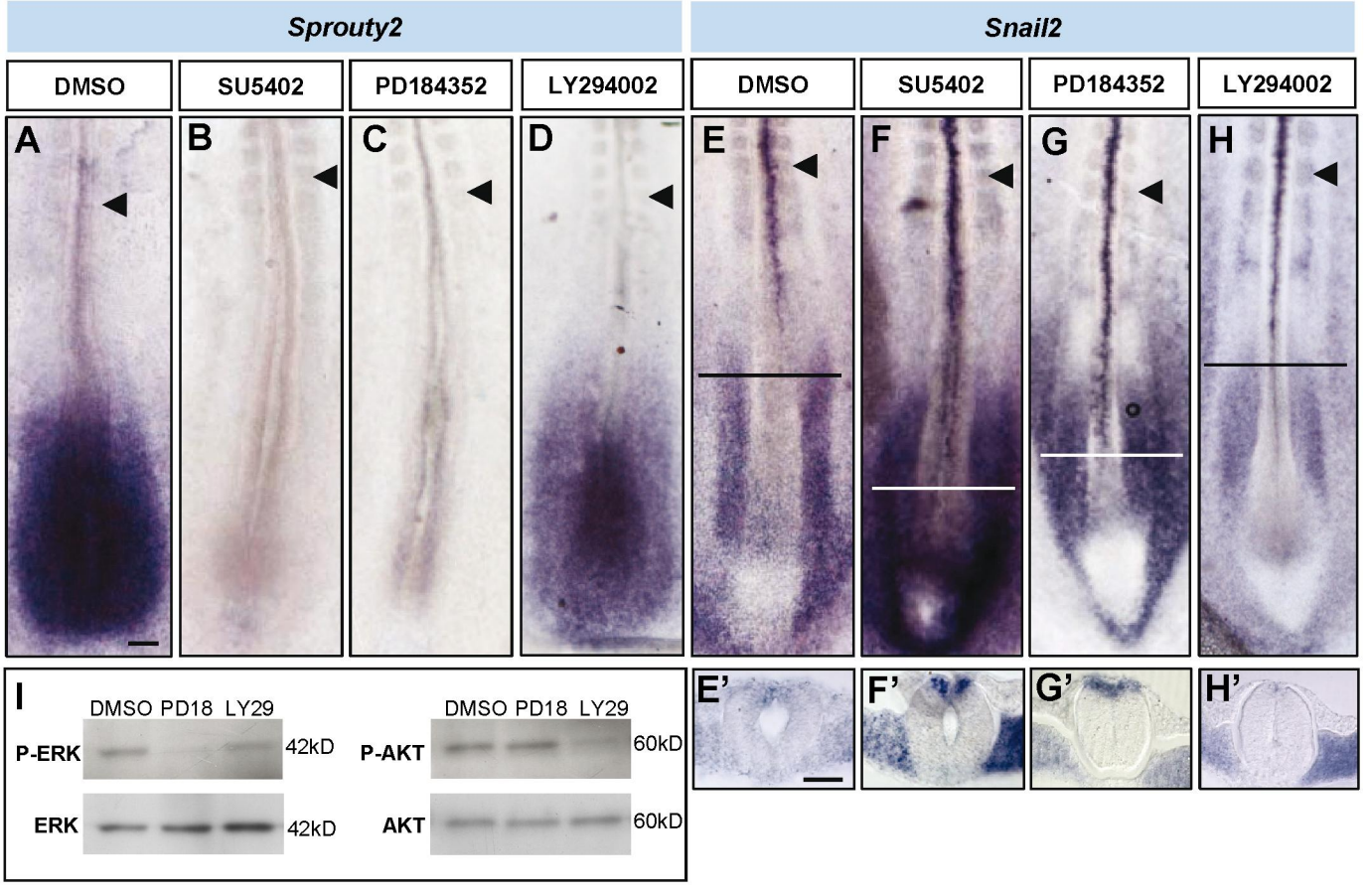

Martínez-Morales et al. Figure 3

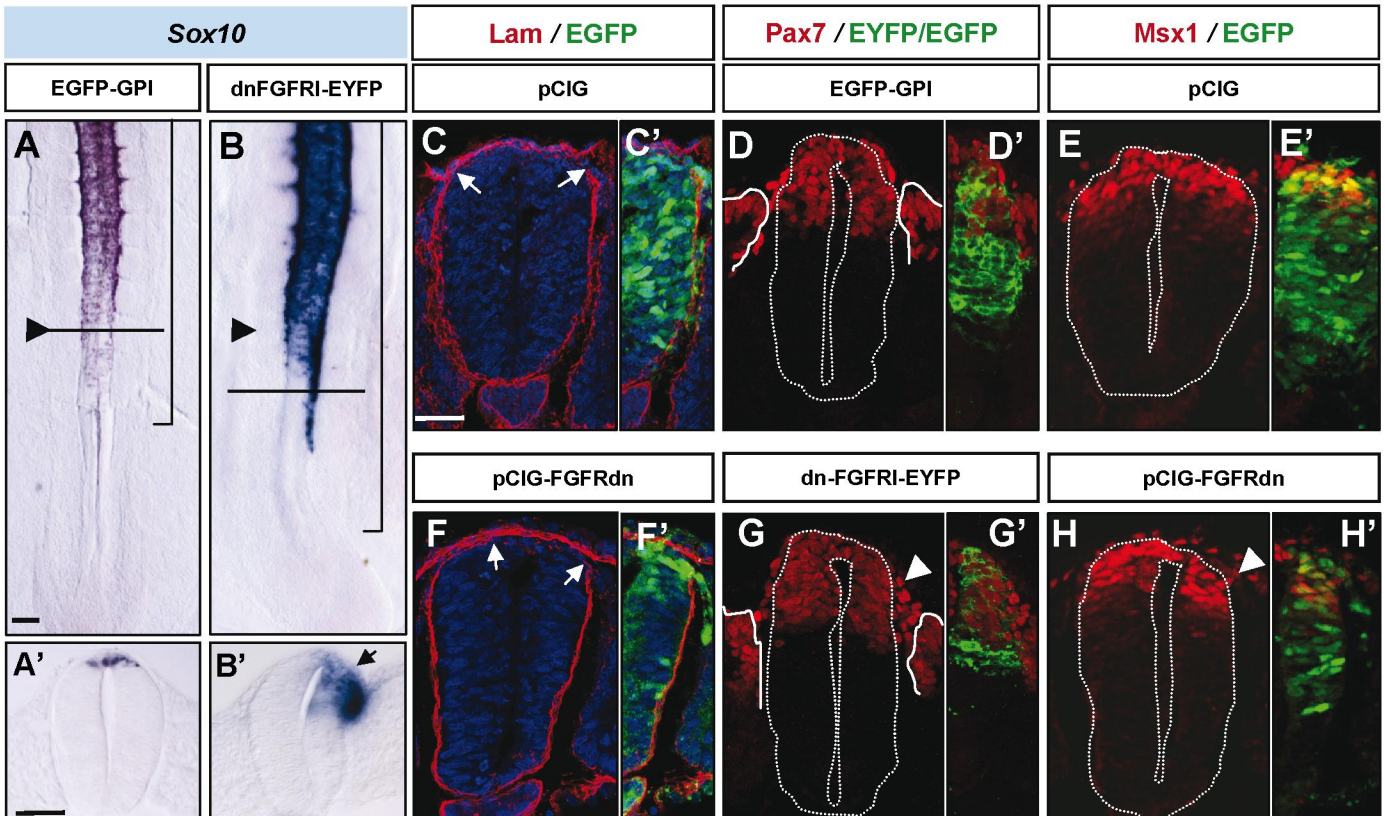

Martínez-Morales et al. Figure 4

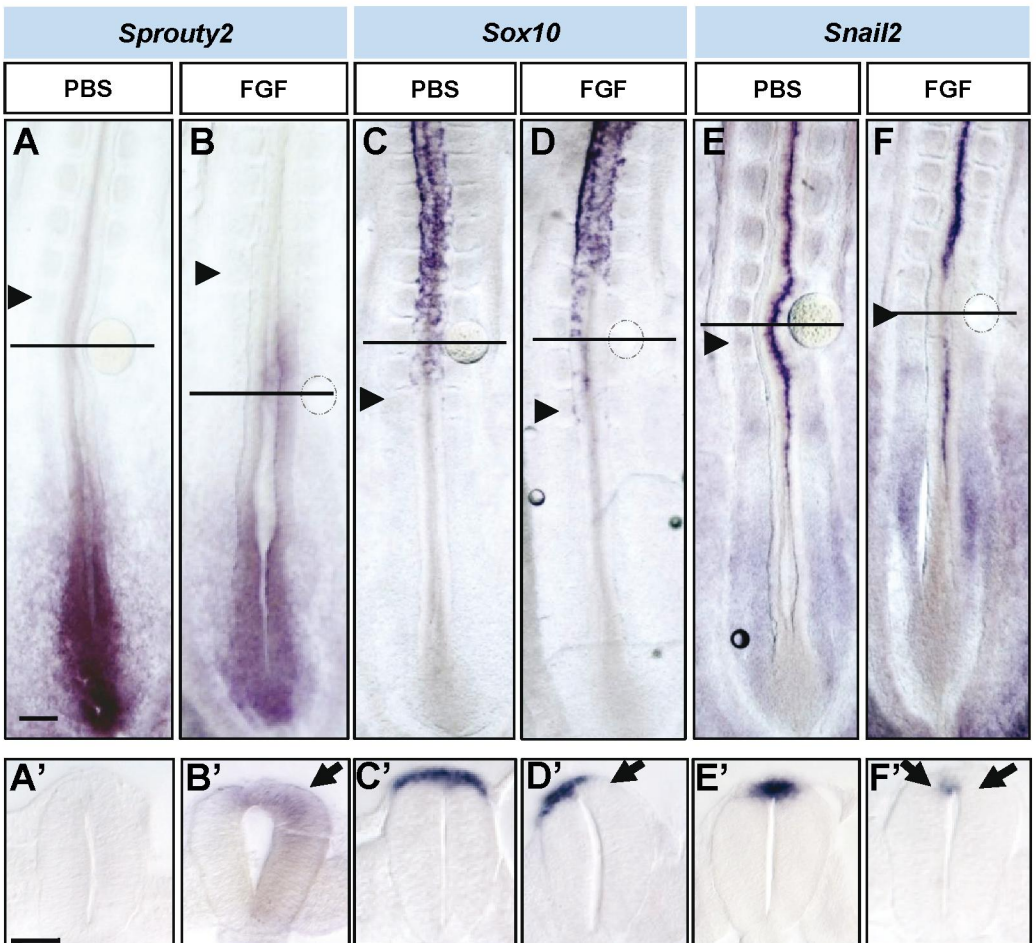

Martínez-Morales et al. Figure 5

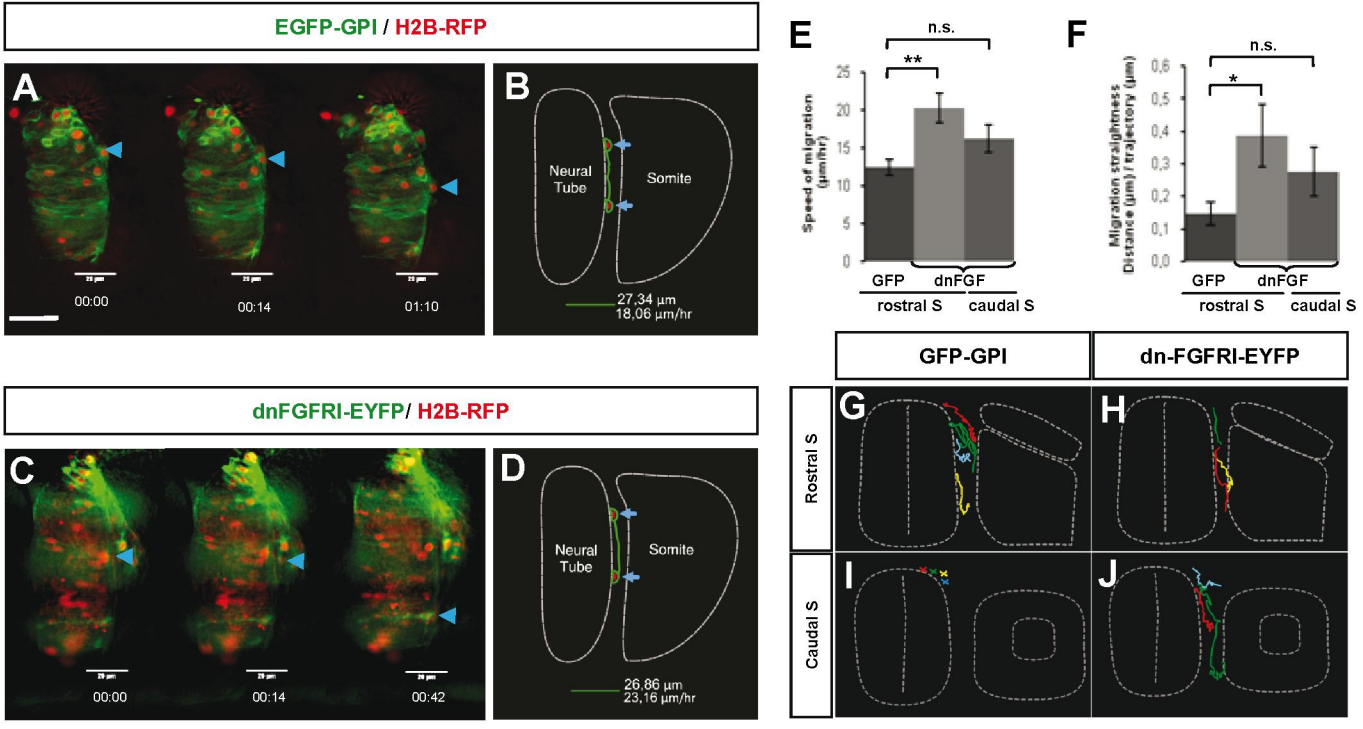

Martínez-Morales et al. Figure 6

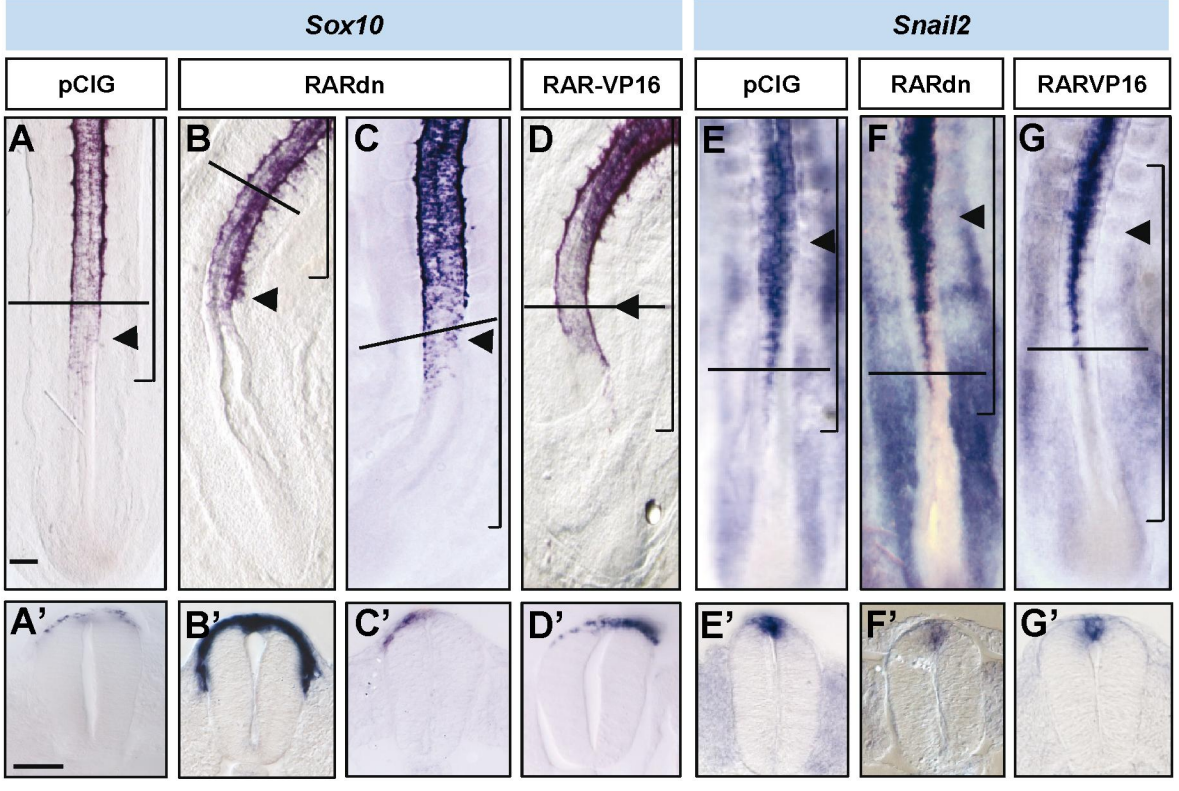

Martínez-Morales et al. Figure 7

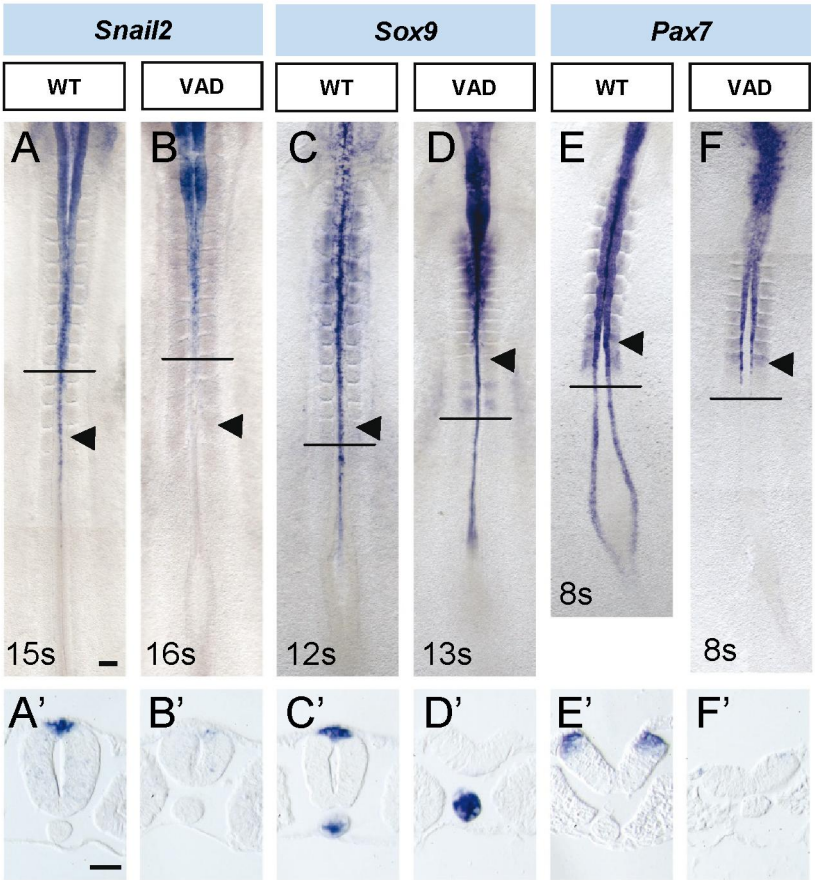

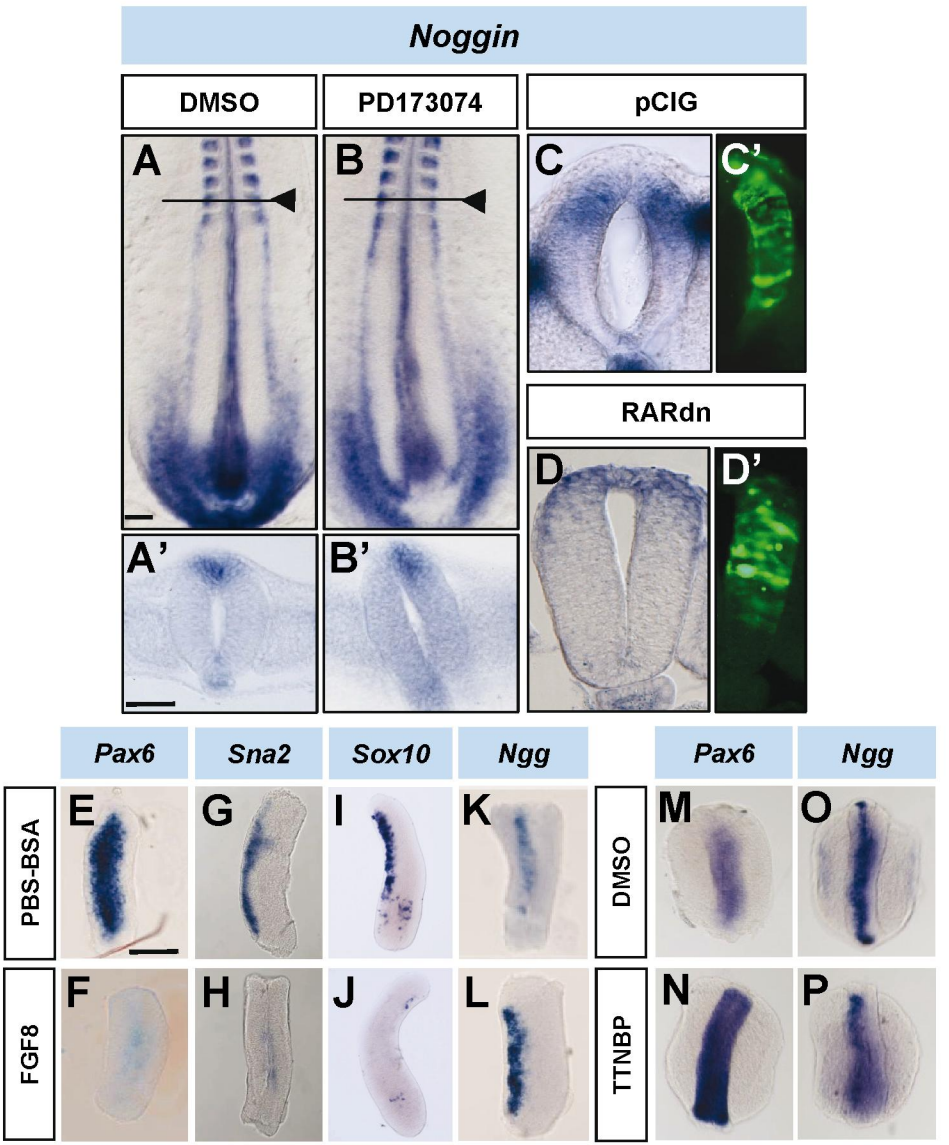
Noggin
DMSO
PD173074
pCIG
A
B
C
C'
A'
B'
RARdn
D
D'
Pax6
Sna2
Sox10
Ngg
Pax6
Ngg
PBS-BSA
DMSO
E
G
I
K
M
O
FGF8
TTNBP
F
H
J
L
N
P

Martínez-Morales et al. Figure 9

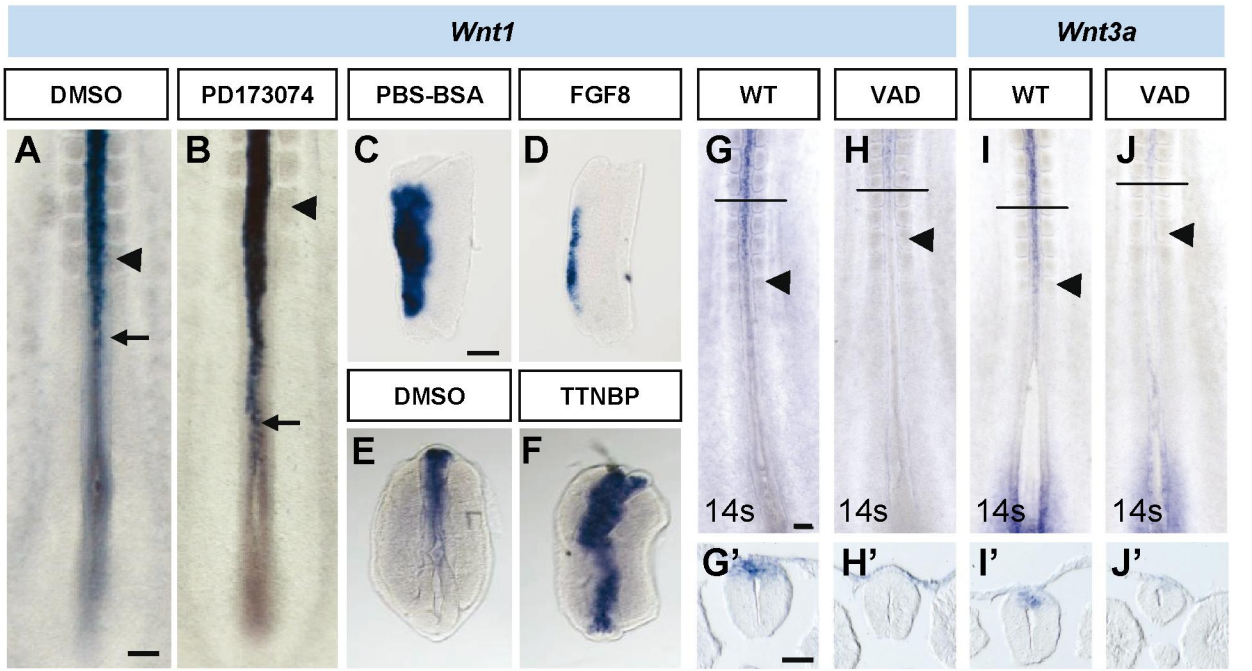

Martínez-Morales et al. Figure 10

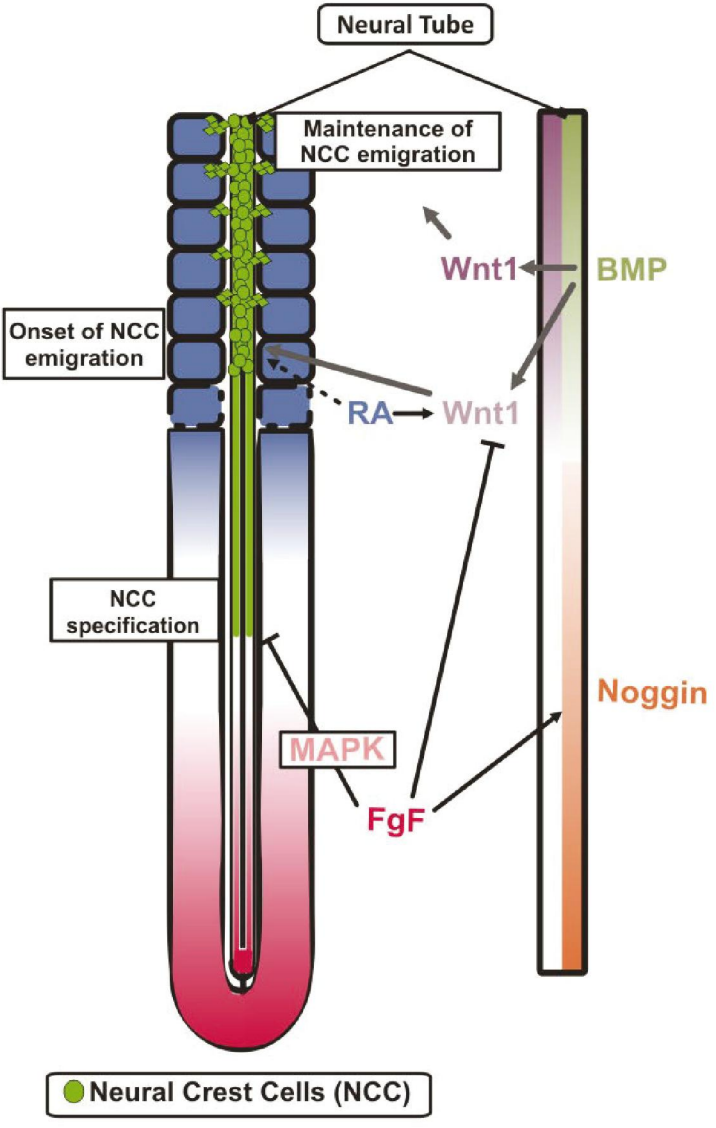

Online supplemental material

Supplementary Figure 1. **Analysis of NCC specification and emigration upon FGFR blockage using the PD173074 inhibitor.** Chicken embryos at stage HH11-12 were cultured for 4 hours in the presence of control (DMSO) or pharmacological inhibitors for FGFRI (PD173074) and were analyzed for the expression of *Sprouty2* (A-B), as a control, and for *Snail2* (C,D), *FoxD3* (E,F) and *Sox10* (G,H). Black arrows point to the last formed somite, white arrows the caudal level of *Snail2* expression in the neural tube and black arrows point to the most caudal level of gene expression in the neural tube. (I) Relative mRNA levels of *Sprouty* and *Snail2* in explants of neural tube together with notochord taken at caudal presomitic mesoderm levels obtained from embryos cultured for 4h. In the presence of PD173074, *Sprouty* levels decrease and *Snail2* levels increase with respect to control samples (DMSO treated). Levels were determined by qRT-PCR and normalized to 18S rRNA. Error bars indicate SD for *Sprouty* (Standard Curve method) and $2^{-\Delta\Delta Ct \pm SD}$ for *Snail2* (Comparative Ct method, see methods section). Significant differences were tested by Student's t-test. (*) $p<0.05$.Scale bar: 200µm.

Supplementary Figure 2. **VEGFR activity inhibition does not alter *Snail2* expression in the neural tube.** (A,B) Chicken embryos at stage HH11-12 were cultured for 4 hours in the presence of control (DMSO; A) or pharmacological inhibitors for VEGFR (KRN633; B) and analyzed for the expression of *Snail2*. Trunk explants at the level of rostral PSM from HH13-14 embryos were culture for 24 hours in the presence of DMSO (C; n=7) or KRN633 (D; n=8) and analysed for *VE-cadherin* expression. Black arrows point to the last formed somite, white arrows the caudal level of *Snail2* expression. Scale bar: 150µm (A,B), 70µm (C,D).

Supplementary Figure 3. **Blockage of FGF signaling pathway promotes premature *Pax6* expression and prevents *Sprouty2* expression in the neural tube.** Stages HH11-13 embryos electroporated on the right neural hemitube with control (EGFP-GPI) or a dominant negative truncated version of FGFRI fused to EYFP (dnFGFRI-EYFP) constructs and analyzed 18-24 hours later. (A-B) *Pax6* expression. (C,D) *Sprouty2* expression. Black arrowheads point the last formed somite, brackets to the electroporated area and black arrows to *Sox10* expression in migratory NCCs. (A'-D') Transverse section at the level indicated by a bar in the corresponding figure. Scale bars: A (for A-D) 45µm; A' (for A'-D') 30µm.

Supplementary Figure 4. **Blockage of FGF signaling pathway promotes NCCs premature emigration of several populations.** Stages HH11-13 embryos electroporated on the right neural hemitube with control pCIF or a dominant negative truncated version of FGFRI in pCIG (pCIG-FGFRdn) constructs and analyzed 18-24 hours later.(A-F) Immunostaining in electroporated embryos showing in red Sox5(A,D), Ap2 (B,E) and Pax7(C,F) expression. (A'-F') EGFP expression in the electroporated hemitube. White arrows in D' points to double GFP^+/ $Sox5^+$ cells. Observe that there is a high number of migratory $Sox5^+$ cells that are GFP^-.(G) Quantification of the number of cells in the electroporated area that expresses a marker respect to the cells expressing the same that marker in an equivalent area in the non electroporated side (% $cells^+$ EP/$cells^+$ C). (H) Quantification of the relative number of migratory $Sox5^+$cells that are either GFP^+ or GFP negative (GFP^-) with respect to the number of $Sox5^+$ migratory cells in the control non electroporated side (as a way of normalization to reduce axial level variations; %cells EP/cells C) in both pCIG or FGFRdn electroporated embryos. Quantitative data were expressed as mean ±s.d. n≥4 embryos (and at least 4 sections per

embryo) per experimental point. Significant differences were tested by Student's test. (*) $p<0.05$; (**) $p<0.01$; (***) $p<0.001$. Scale bar: 30 μm.

Supplementary Figure 5. **RA signaling is not required to maintain NCC emigration. RA signaling does not control the onset of FoxD3 expression in the neural tube** Chicken embryos at stages HH11-13 were electroporated on the right neural hemitube with control pCIG construct or a dominant negative truncated version of RARα in pCIG (RARdn) at rostral somatic levels and analyzed 18-24 hours later. (A-C) Inmunostaining for Pax6 showing a clear reduction in PCIG-RARdn electroporated neuroepithelial cells. (B,D) $AP2^{+}$ pre- and migratory NCCs are not affected by the blockage in RA signaling pathway. (A'-D') GFP electroporated areas.(E-G) Chicken embryos at stages HH11-13 electroporated on the right neural hemitube with control pCIG, RARdn or a constitutively active form of the RARα (RAR-VP16) and analyzed 18-24 hours later for *FoxD3* expression. Black arrowheads point the last formed somites and brackets to the electroporated area. (E'-G') Transversal section at the level indicated by a bar. Scale bar: for A-D, 25μm; for E-G, 180μm; for E'-G', 40μm.

Fig5video1. Movie showing the migration of NCCs electroporated with H2B-RFP (red) and with control EGFP-GPI (green) at the level of differentiating somites (V-XII somites). Cells were imaged by time-lapse microscopy using a Delta Vision Core microscope (Applied Precision, LLC, Issaquah, WA) and images were taken at 7 min interval. A total of 104 frames were taken during 12 hours.

Fig5video2. Movie showing the migration of NCCs electroporated with H2B-RFP (red) and with dnFGFR1-EYFP (green) at the level of differentiating somites (V-XII somites). Cells were imaged by time-lapse microscopy using a Delta Vision Core

microscope (Applied Precision, LLC, Issaquah, WA) and images were taken at 7 min interval. A total of 63 frames were taken during 7.5 hours.

Fig5video3. Movie showing the migration of NCCs electroporated with H2B-RFP (red) and with dnFGFR1-EYFP (green) at the level of epithelial somites (I-IV somites). Cells were imaged by time-lapse microscopy using a Delta Vision Core microscope (Applied Precision, LLC, Issaquah, WA) and images were taken at 7 min interval. A total of 99 frames were taken during 12 hours.

Martínez-Morales et al. Supplementary Figure 1

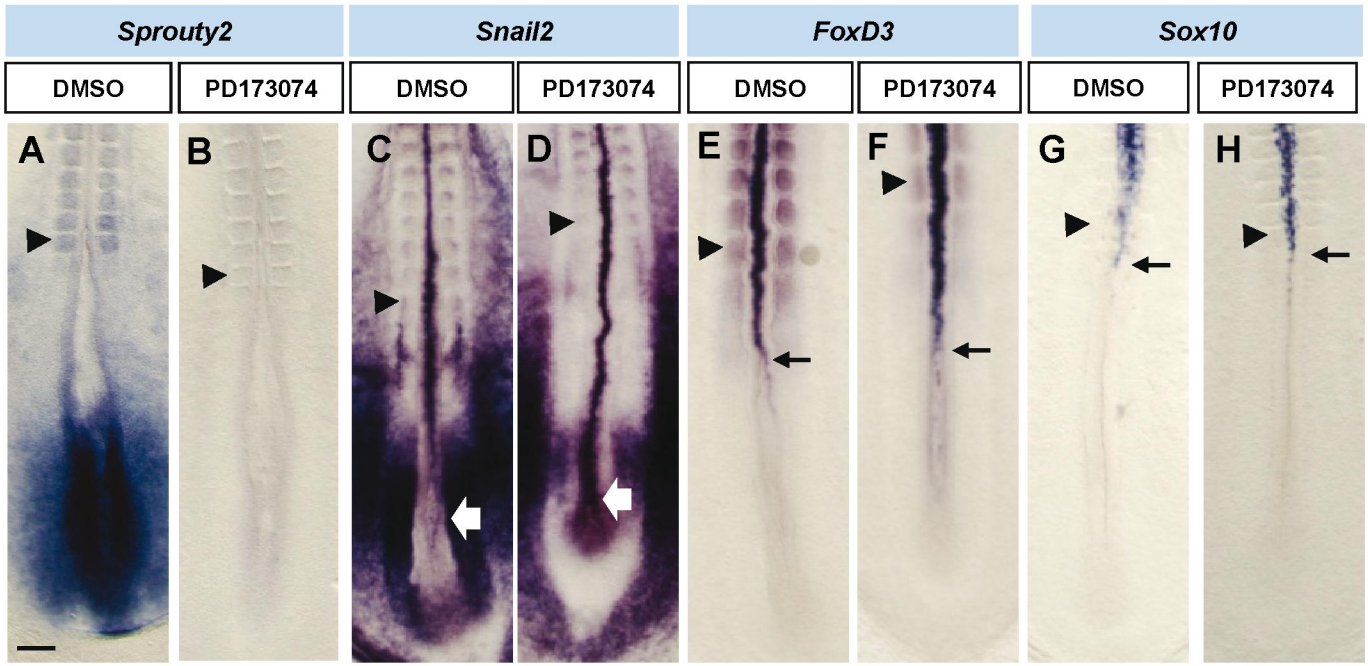

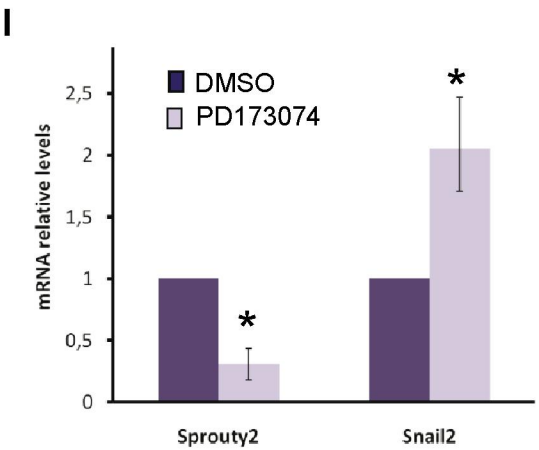

Martínez-Morales et al. Supplementary Figure 2

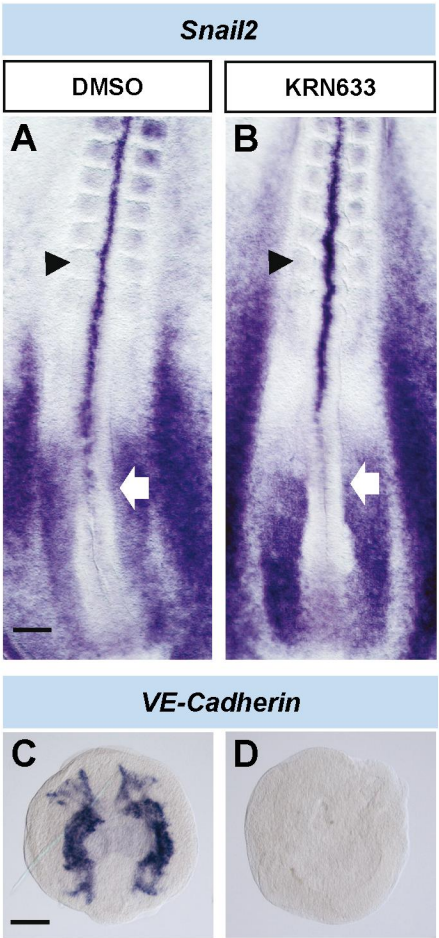

Martínez-Morales et al. Supplementary Figure 3

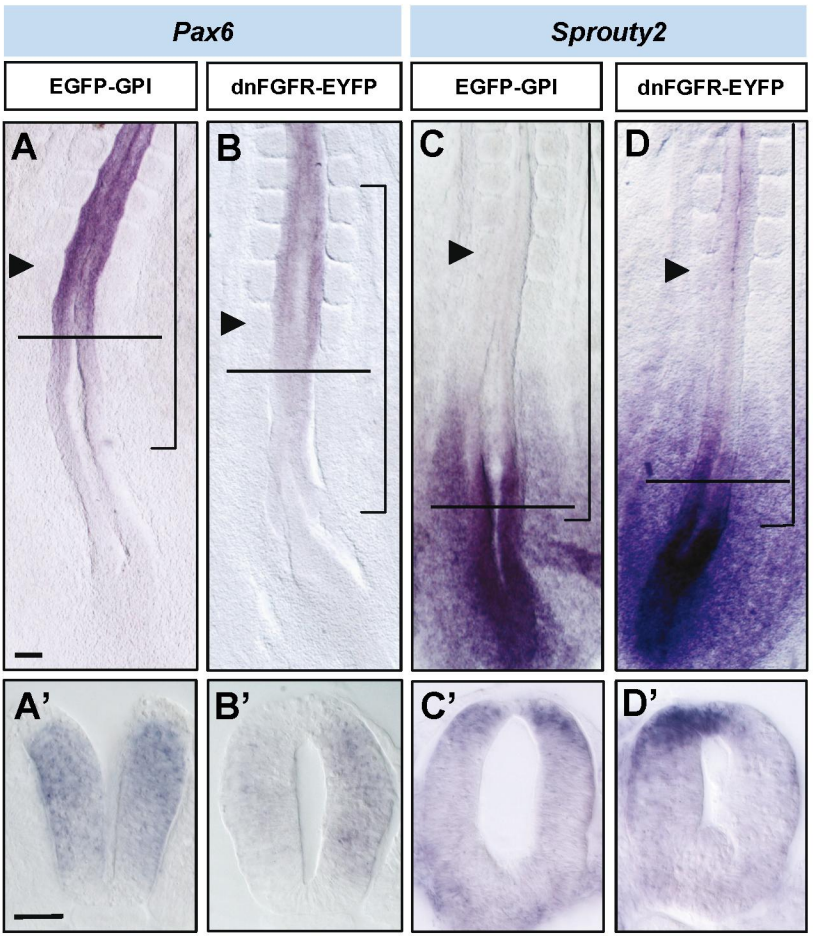

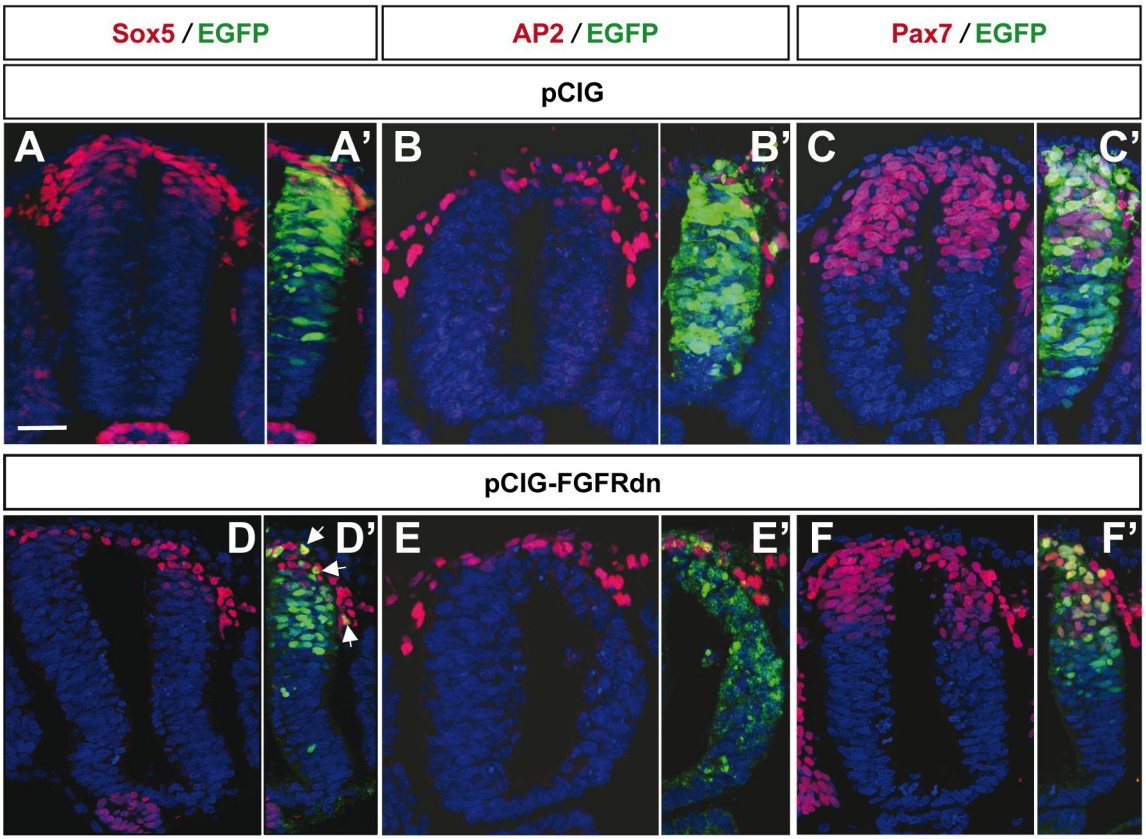
Sox5 / EGFP
AP2 / EGFP
Pax7 / EGFP
pCIG
A
A'
B
B'
C
C'
pCIG-FGFRdn
D
D'
E
E'
F
F'

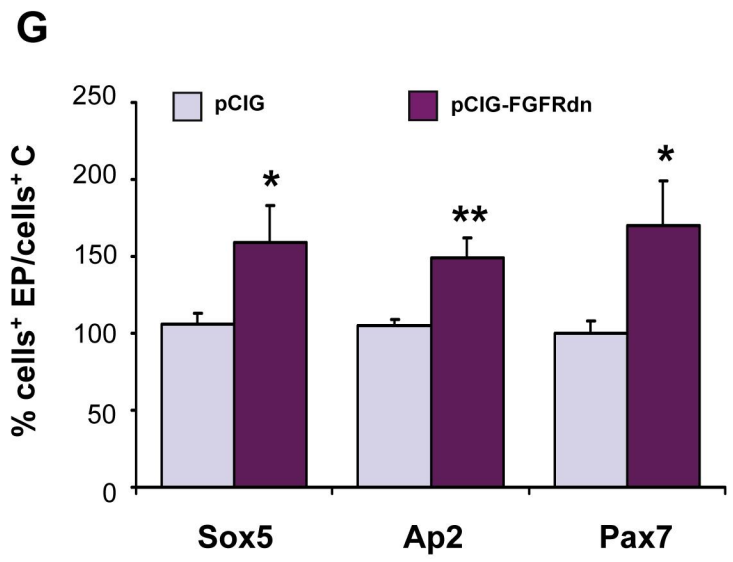
G
% cells+ EP/cells+ C
250
200
150
100
50
0
pCIG
pCIG-FGFRdn
*
**
*
Sox5
Ap2
Pax7

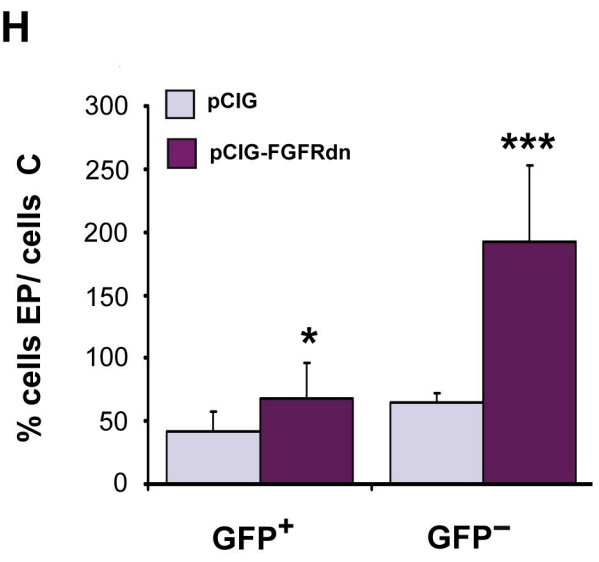
H
% cells EP/ cells C
300
250
200
150
100
50
0
pCIG
pCIG-FGFRdn
*
***
GFP+
GFP−

Martínez-Morales et al. Supplementary Figure 5